

# Genome mining and UHPLC–QTOF–MS/MS illuminate the potential antimicrobial active compounds and specificity of biosynthetic gene clusters in *Bacillus subtilis* NCD-2

**Zhenhe Su**

Hebei Academy of Agriculture and Forestry Sciences

**Xiuye Chen**

Hebei Academy of Agriculture and Forestry Sciences

**Xiaomeng Liu**

Hebei Academy of Agriculture and Forestry Sciences

**Qinggang Guo**

Hebei Academy of Agriculture and Forestry Sciences

**Shezeng Li**

Hebei Academy of Agriculture and Forestry Sciences

**Xiuyun Lu**

Hebei Academy of Agriculture and Forestry Sciences

**Xiaoyun Zhang**

Hebei Academy of Agriculture and Forestry Sciences

**PeiPei Wang**

Hebei Academy of Agriculture and Forestry Sciences

**Lihong Dong**

Hebei Academy of Agriculture and Forestry Sciences

**Weisong Zhao**

Hebei Academy of Agriculture and Forestry Sciences

**Ping Ma** (✉ [pingma88@126.com](mailto:pingma88@126.com))

Institute of Plant Protection

---

## Research article

**Keywords:** Bacillus subtilis NCD-2, Genome mining, UHPLC–QTOF–MS/MS, Secondary metabolites, Fengycin

**Posted Date:** August 13th, 2020

**DOI:** <https://doi.org/10.21203/rs.3.rs-33091/v2>

**License:** © ⓘ This work is licensed under a Creative Commons Attribution 4.0 International License. [Read Full License](#)

---

**Version of Record:** A version of this preprint was published at BMC Genomics on November 5th, 2020. See the published version at <https://doi.org/10.1186/s12864-020-07160-2>.

## Abstract

Background *Bacillus subtilis* strain NCD-2 is an excellent biocontrol agent against plant soil-borne diseases and shows broad-spectrum antifungal activities. This study aimed to explore some of the secondary metabolite biosynthetic gene clusters and related bioactive compounds in strain NCD-2. An integrative approach, which combined genome mining with structural identification technologies using ultra-high-performance liquid chromatography coupled to quadrupole time-of-flight tandem mass spectrometry (UHPLC-MS/MS), was conducted to interpret the chemical origins of the significant biological activities in strain NCD-2. Results Genome mining revealed that strain NCD-2 contained nine gene clusters having predicted functions involving secondary metabolites with bioactive abilities. They encoded six known products including fengycin, surfactin, bacillaene, subtilosin, bacillibactin, bacilysin and three unknown products. Fengycin, surfactin, bacillaene and bacillibactin were successfully detected from the fermentation broth of strain NCD-2 by UHPLC-QTOF-MS/MS. Bacillaene, subtilosin, bacillibactin, and bacilysin related biosynthetic gene clusters showed 100% amino acid sequence similarity with *B. velezensis* strain FZB42—however, the biosynthetic gene clusters for surfactin and fengycin showed 83% and 92%, respectively. Further comparison of gene clusters encoding fengycin and surfactin revealed that strain NCD-2 had lost the *fenC* and *fenD* genes in the fengycin biosynthetic operon. Moreover, biosynthetic enzyme-related gene *srfAB* for surfactin had divided into two parts. Bioinformatics analysis predicted that *FenE* function in strain NCD-2 was same to that of *FenE* and *FenC* in strain FZB42, and *FenA* function in strain NCD-2 was same to that of *FenA* and *FenD* in strain FZB42. Five kinds of fengycin, with 26 homologs, and surfactin, with 4 homologs, were detected from strain NCD-2. To the best of our knowledge, this is the first report of a non-typical and unique gene cluster related to fengycin synthesis. Conclusions It was found that there were many gene clusters encoding antimicrobial compounds in the genome of strain NCD-2, and the fengycin synthetic gene cluster might be unique by using genome mining and UHPLC-QTOF-MS/MS. The production of fengycin, surfactin, bacillaene and bacillibactin might explain the biological activities of strain NCD-2.

## Background

*Bacillus subtilis* and its closely related species are ubiquitous inhabitants of soil, and are widely recognized as powerful biocontrol agents against plant soil-borne diseases [1]. The *Bacillus* genus has received considerable attention as a biological resource used in the development of microbial pesticides, in part because some or most of its members form stress-resistant spores that do not harm the environment and are useful in pesticide production [2-4]. The mechanisms used by *B. subtilis* to suppress plant soil-borne diseases include competing with phytopathogens for nutrients and spatial sites, inducing the systemic resistance of plants, and inhibiting pathogen growth by producing antimicrobial compounds [5]. The latter is a general characteristic of *B. subtilis* biocontrol capability and plays an important role in the biological control of plant diseases [6, 7]. *B. subtilis* produces more than two dozen antimicrobial compounds having amazing structural variety. On the basis of the biosynthetic pathway, the antimicrobial compounds are divided into small molecular compounds synthesized by the ribosomal pathway, such as bacteriocins, and peptide compounds synthesized by the non-ribosomal pathway, such as lipopeptides and polyketides [8]. Most antimicrobial compounds are secondary metabolites, with very complex chemical structures, that are not necessary for the growth and reproduction of microorganisms. Secondary metabolites function as essential chemical signals for the induction of cellular differentiation in the producing organism and for controlling its metabolism [9, 10]. They also function as antibiotics, and their antimicrobial properties may lead to shifts within rhizospheric microbial functional subsystems, such as affecting the availability of nutrients for the plant [11].

The genes encoding the secondary metabolites commonly exist in clusters and encode complex enzymes with multiple functions [12]. The polyketide synthase/non-ribosomal peptide synthetase (PKS/NRPS) gene clusters have been well studied. The PKS pathway polyketides require at least three domains, an acyl transferase, a ketosynthase, and an acyl carrier protein [13]. The NRPS pathway shares a common mode of synthesis, the multicarrier thiotemplate mechanism, requiring the cooperation of three basic domains [14]. The adenylation domain selects its cognate amino acid and generates an enzymatically stabilized aminoacyl adenylate. The peptidyl carrier domain is equipped with a 4'-phosphopantetheine prosthetic group to which the adenylated amino acid substrate is transferred and bonded by a thioester bond. The condensation domain catalyzes the formation of a new peptide bond [13]. The carbon skeleton in the metabolite is synthesized by the core PKS and

Loading [MathJax]/jax/output/CommonHTML/jax.js

NRPS enzymes, and then, the final product is formed with the assistance of various modifying enzymes [15]. The bioactive secondary metabolites produced by the PKS/NRPS pathway in species of *B. subtilis* include bacilysin [16], bacilysocin [17], surfactin [18], iturin A [19], fengycin [20], mycosubtilin [21], bacillomycins [8], and difficidin [16].

The traditional method of screening for new active products is based on testing for biological activity. However, this method is time-consuming and the same products have been repeatedly discovered [22]. Thus, the discovery of natural products had encountered a bottleneck [23], and the development of a more rapid and effective screening strategy to detect new secondary metabolites was necessary [24, 25]. Genome mining is a technology that uses modern bioinformatics to recognize specific functional genes or gene clusters from genome sequences [26]. With the rapid development of gene sequencing technology and the decreasing cost of genome sequencing, increasing numbers of microbial genome sequences have been determined [27]. Therefore, genome mining has become a more accurate and efficient screening strategy for discovering new metabolites [26].

*B. subtilis* strain NCD-2 is a promising biological control agent against plant soil-borne diseases that produces lipopeptides, fengycin, and surfactin [28]. Fengycin has an antifungal activity, and surfactin facilitates the root colonization ability of strain NCD-2. Both fengycin and surfactin play important roles in strain NCD-2's ability to suppress plant soil-borne diseases [29]. The purpose of this study was to identify potential secondary metabolites in strain NCD-2 using genome mining. Then, bioinformatics analysis was conducted to reveal the differences between gene clusters for these secondary metabolites in strain NCD-2 and reference strain *B. velezensis* FZB42. Finally, ultra-high-performance liquid chromatography coupled to quadrupole time-of-flight tandem mass spectrometry (UHPLC-QTOF-MS/MS) was used to identify the potential secondary metabolites produced by strain NCD-2.

## Results

### Genomic features of strain NCD-2

A total of 501,671,500 paired-end reads and 5,016,715 clean single reads (412-bp library; paired-ends of 75 bp) were assembled using the software Velvet [30]. The genome of *B. subtilis* NCD-2 contained 189 contigs (>133 bp; N90, 16,187) of 4,644,322 bp, with an average G+C content of 43.5%. The final assembled genome comprised 4,444 genes, including 4,329 protein-coding genes (418 signal peptide-coding genes), 83 tRNA genes for all 20 amino acids, 30 rRNA genes, and 2 CRISPR repeat genes. A total of nine putative gene clusters responsible for antimicrobial metabolite biosynthesis were identified. These gene clusters included PKS and NRPS genes (Fig. 1).

### The taxonomic status of strain NCD-2

At present, 272 *B. subtilis* genome sequences were deposited in the GenBank database, including 113 whole- and 159 incomplete genome sequences. The genome sizes of the 272 *B. subtilis* strains ranged from 2.68 Mb to 5.35 Mb, and the GC contents ranged from 42.9% to 46.6%. These genome sequences were downloaded from the GenBank database, and their accession numbers were listed (Additional file 1, Table S1). To analyze the evolution of different *B. subtilis* strains, a phylogenetic tree was constructed based on the complete genome sequences. The 272 strains of *B. subtilis* were divided into four subspecies, *subtilis*, *inaquosorum*, *spizizenii*, and *stercoris* because of producing different bioactive secondary metabolites [31]. As shown in Fig. 2, strain NCD-2 (represented by the black bar) clustered together with *B. subtilis* strain UD1022 and was closely related to *B. subtilis* strains XF-1, BAB-1, HJ5, SX01705, and BSD-2.

### Secondary metabolite biosynthetic gene clusters in strain NCD-2

The secondary metabolite biosynthetic gene clusters in the genome of strain NCD-2 were predicted using the online website antiSMASH [32]. In total, nine secondary metabolic gene clusters were identified in the NCD-2 genome sequences (Table 1), including three NRPS, two terpenes, one heterozygous NRPS-TransAT PKS-Other KS, one type III polyketide, one sactipeptide-head to tail gene cluster, and a gene cluster with an unknown function. The structural compositions of the gene clusters were

Loading [MathJax]/jax/output/CommonHTML/jax.js

other genes. Among these nine gene clusters, clusters 3, 7, 8, and 9 had 100% amino acid sequence homology with known gene clusters that synthesize bacillaene, bacillibactin, subtilosin, and bacilysin, respectively (Table 1). Gene cluster 1 showed 82% amino acid similarity with a surfactin synthetase gene cluster, and gene cluster 4 showed 93% amino acid similarity with a fengycin biosynthetic gene cluster in *B. velezensis* strain FZB42. However, gene clusters 2, 5, and 6 did not match any known gene clusters. Clusters 1 and 4 of strain NCD-2 were further compared with those of the model strain 168 and *B. subtilis* strains closely related phylogenetically to strain NCD-2. The fengycin potentially being coded by biosynthetic gene cluster of strain NCD-2 contained three genes, *fenEAB*, while the other strains contained five genes, *fenCDEAB* (Additional file 1, Fig. S1). SrfAB of surfactin was synthesized by the typical transcription and translation of *srfAB* in the 11 strains. However, the same SrfAB was potentially assembled with Gms0366 and Gms0367 and then transcribed and translated by *gms0366* and *gms0367* separately in strain NCD-2 (Additional file 1, Fig. S2). Therefore, we hypothesized that the structures and functions of fengycin and surfactin from strain NCD-2 may be different from those of the other *B. subtilis* strains.

### Specificity of surfactin and fengycin synthetase gene clusters in *B. subtilis* NCD-2

The surfactin biosynthetic gene cluster in strain NCD-2 was analyzed using PRISM, and the core genes were selected for a PKS/NRPS analysis. This gene cluster contained four genes: *gms0365*, *gms0366*, *gms0367*, and *gms0368*. Gms0365 showed an identical conserved structural and functional domain, CATCATCATe, with SrfAA in strain FZB42, in which C, A, T, and Te represent the condensation, adenylation, thiolation, and thioesterase domains, respectively (Fig. 4a). Compared with SrfAB in strain FZB42, Gms0366 in strain NCD-2 had lost the T and E domains, but the amino acid residues for the binding pockets of Gms0366 were exactly the same as those of SrfAB. The residues of the different adenylation domains A6 and A2 from the enzymes Gms0365 and Gms0366, respectively, were exactly the same, and both bound the amino acid leucine. Gms0367 had only T and E domains, with no specific substrate-binding domain. The superposition of Gms0367 and Gms0366 domains formed a complete SrfAB. The T domain was reversed between Gms0367 and Gms0368. The domains of Gms0368 were CATe, in which the thioesterase domain released linear peptide chains. The domains of Gms0368 were exactly the same as those of SrfAC, but the amino acid residues forming the binding pockets were not completely conserved. The residue sequence was DAF-LGCV, compared with DAFXLGCV of strain FZB42, revealing a difference of one residue.

The fengycin biosynthetic gene cluster was analyzed by PRISM, and the core genes were selected for a PKS/NRPS analysis. This cluster contained five genes in strain FZB42's genome, they were ordered as *fenCDEAB* (Fig. 4b). However, according to Fig.4b, the fengycin biosynthetic gene cluster in strain NCD-2 contained only three genes: *gms1961*, *gms1960*, and *gms1959*. Gms1961 of strain NCD-2 corresponded to FenE in strain FZB42 had conserved residues of A8 and A9, which bound two amino acids Glu and Val, respectively (Fig. 4b). Gms1960 and Gms1959 in strain NCD-2 had conserved amino acids sequences related to FenA and FenB in strain FZB42, respectively. Interestingly, no homologs of FenC and FenD were identified in the genome of strain NCD-2. Consequently, the amino acid sequences of FenC and FenD from strain FZB42 were compared with the strain NCD-2 proteome using BioEdit. Gms1961 was most similar to FenC, and Gms1960 was most similar to FenD (Additional file 1, Tables. S2, S3). Therefore, it was hypothesized that Gms1961 and Gms1960 performed the functions of FenC and FenD in strain NCD-2, respectively. Thus, Gms1961 and Gms1960 might have dual functions, in details, Gms1961 in strain NCD-2 served as FenE and FenC in strain FZB42, Gms1960 in strain NCD-2 served as FenA and FenD in strain FZB42, in the synthesis of fengycin. However, the FenD domain varied greatly between strain NCD-2 and FZB42, and other enzymes might have similar function as FenD.

To further confirm the unique structure of fengycin synthetase gene cluster in strain NCD-2, a pair of primers that binding the *fenE* and *dacC* were designed, the binding sites were identical between strain NCD-2 and FZB42 (Fig. 5a). With the primers set, a 4791 bp fragment was successfully amplified from strain NCD-2, but failed to amplify target the fragment from strain FZB42 due to the larger target fragment (20290 bp) in it (Fig. 5b). The amplicon from strain NCD-2 was purified and ligated to pEASY-Blunt Zero vector (Fig. 5c), and then was sequenced. The sequences alignment confirmed that *fenC* and *fenD* were deficient in strain NCD-2 (Fig.5d). The role of *gms1961* in the fengycin production was also tested. Strain NCD-2 could produce abundant fengycin, however, the in-frame deletion of *gms1961* in strain NCD-2 completely lost the fengycin production (Fig. 6a-c).

To further investigate whether the structure of the fengycin synthetase gene cluster in NCD-2 was strain specific, the fengycin biosynthetic gene clusters from 11 different *B. subtilis* strains that were closely related to strain NCD-2 or are model strains were compared (Additional file 1, Fig. S1). The gene cluster sequences of all 11 strains were *fenCDEAB* (also *ppsABCDE*), and only that of strain NCD-2 was *fenEAB*. Therefore, the fengycin biosynthetic gene cluster of strain NCD-2 is unique.

### MS/MS of fengycin and surfactin in NCD-2

Fengycin was separated from the lipopeptide extract of strain NCD-2 using Fast protein liquid chromatography (FPLC) (Additional file 1, Fig. S3), and the QTOF-MS/MS analysis revealed five fractions in the fengycin cluster (Fig. 7a–e). The five fractions had mass-to-charge ratio ( $m/z$ ) values of 732.4, 746.4, 725.4, 739.4, and 767.4 (secondary MS), representing fengycin A, fengycin B, fengycin A2, fengycin B2, and fengycin C, respectively. The typical MS/MS spectra showed the distributions of key fragmentation ions ( $\alpha$  and  $\beta$ ), representing the linear N-terminal and the cyclic C-terminal segments, respectively, of diverse fengycin species (Additional file 1, Fig. S4a–b) and (Fig. 7a–e). The MS/MS spectrum of the fengycin ion at  $m/z$  732.4 yielded two intense product ions at  $m/z$  966.5 and 1,080.5, representing fengycin A (Fig. 5a), while the MS/MS spectrum of the fengycin ion at  $m/z$  746.4 (Fig. 7b) yielded key product ions at  $m/z$  994.5 and 1,108.6, representing fengycin B (Fig. 7b). The MS/MS spectrum of the fengycin ion at  $m/z$  725.4 yielded two intense product ions at  $m/z$  952.4 and 1,066.5, representing fengycin A2 (Fig. 7c), while the MS/MS spectrum of the fengycin ion at  $m/z$  739.4 (Fig. 7d) yielded key product ions at  $m/z$  980.5 and 1,094.5 representing fengycin B2 (Fig. 7d). The MS/MS spectrum of the fengycin ion at  $m/z$  767.4 yielded two intense product ions at  $m/z$  994.5/1,008.5 and 1,108.6/1,122.6 representing fengycin C (Fig. 7e). Five classes of fengycins were identified based on the key product ions of  $\beta$ -hydroxy fatty acid ( $\beta$ -OH FA) with chain lengths varying from C12 to C20 (Table 2, Figs. S5–S9). The MS/MS spectrum of the surfactin ion at  $m/z$  1,008.7 yielded one intense product ion at  $m/z$  685.5 (Fig. 7f; Additional file 1, Fig. S4c). Based on these key product ion, one class of surfactin was identified, which were the surfactins ( $m/z$  values of 994.6, 1,008.7, 1,022.7 and 1,036.7) of fatty acids with chain lengths varying from C11 to C15 (Fig. S10).

### Detection of other antimicrobial active compounds in NCD-2

Except for the fengycin and surfactin, bacillaene, bacilysin, bacillibactin and subtilosin were also predicted from the genome of strain NCD-2. The four predicted antimicrobial active compounds were extracted from the fermentation broth of strain NCD-2 by using different extracting methods, respectively. However, only bacillaene and bacillibactin were detected from the extracts by UHPLC-QTOF-MS (Fig. 8a, 8b).

## Discussion

Species of *B. subtilis* have the potential to produce two dozen antimicrobial substances, and 5%–8% of the *B. subtilis* genome contributes to the production of antimicrobial substances [33]. Some inhibit the growth of pathogens and the germination of spores. The lipopeptide mixture of *B. subtilis* C232 inhibits the formation of *Verticillium dahliae* microsclerotia [34], and the volatile compounds secreted by *B. subtilis* JA inhibit the conidial formation and mycelial growth of *Glomus etunicatum* [35].

However, certain bioactive compounds are synthesized only under special conditions or as the result of external stimulation; therefore, it is difficult to obtain all the antimicrobial compounds produced by *Bacillus* using traditional cultivation and extraction methods, and this limited the comprehensive understanding of the mechanisms of biological control and biocontrol bacteria [22]. Genome mining allows the prediction of metabolites based on genome sequences and is widely used in obtaining new antibiotics [26]. It was used to identify a new NRPS pathway product, coelichelin, in *Streptomyces coelicolor* [36].

Pseudomycoicidin in *Bacillus pseudomycooides* DSM 12442 was discovered through the heterologous expression of its BGC in *Escherichia coli* [37]. Traditional cultivation and extraction methods were used to identify lipopeptide, fengycin, and surfactin from *B. subtilis* NCD-2, and fengycin showed strong antifungal abilities against *V. dahliae* and *B. cinerea*. In this study, genome mining was conducted to analyze the potential antimicrobial compounds of the strain NCD-2, and some of them were identified using MS/MS. In total, nine kinds of secondary metabolite gene clusters related to surfactin, bacillaene, fengycin, bacillibactin, subtilosin, bacilysin, two terpenes, and one unknown product were identified from the genome of strain NCD-2. Surfactin

exhibited antibacterial, antiviral, antitumor and hemolytic action [38]. Bacillaene was active compound which could inhibit growth of bacteria by inhibiting prokaryotic protein synthesis [39]. Fengycin showed specific antifungal activity against filamentous fungi [40]. Bacillibactin was siderophore that could uptake iron especially when iron was scarce, *B. subtilis* expressed genes involved in the synthesis for bacillibactin to pirate other microbial siderophores.[41]. Subtilosin possessed antibacterial activity against a diverse range of bacteria [42]. Bacilysin was active compound which showed antibacterial against a wide range of bacteria and *Candida albicans* [43]. They showed antimicrobial abilities and played different roles in suppressing plant diseases. However, only the fengycin, surfactin bacillaene and bacillibactin were successfully detected from the extract of strain NCD-2 by UHPLC-MS/MS (Fig. 7, 8). The bacilysin and subtilosin could not be detected, and it maybe caused by low expression level of biosynthetic gene clusters under the experimental conditions.

*B. velezensis* FZB42 is a model strain of plant beneficial rhizobacteria. 13 gene clusters involved in non-ribosomal and ribosomal synthesis of secondary metabolites with putative antimicrobial action have been identified within the genome of strain FZB42, including fengycin. The mechanism of fengycin synthesis has been well studied in *B. velezensis* strain FZB42 [48]. *B. subtilis* 168 has the entire gene cluster for synthesizing fengycin, but it couldn't produce fengycin because of deficient of a native *sfp* gene [49]. The BGC repository MIBiG (Minimum Information about a Biosynthetic Gene cluster) just has one fengycin biosynthetic gene cluster from *B. velezensis* FZB42 [50, 51]. Therefore, the fengycin biosynthetic gene cluster of strain NCD-2 was compared with that of *B. velezensis* FZB42. Fengycin comprises a peptide ring circled by 10 amino acids with a fatty acid chain tail. The fengycin biosynthetic gene cluster in the strain consists of five genes (38 kb) that encode the synthetases FenCDEAB, of which FenC recognizes and carries glutamate and ornithine, FenD recognizes and carries tyrosine and threonine, FenE recognizes and carries glutamate and valine, FenA recognizes and carries proline, glutamine, and tyrosine, and FenB recognizes and carries isoleucine. FenCDEAB recognizes 10 amino acids and carries them to the  $\beta$ -OH FA chain to form fengycin [52-54]. However, NCD-2 only had *fenEAB*, lacking *fenC* and *fenD*, compared with the typical cluster structure of *fenCDEAB* in the FZB42 strain and 10 other *Bacillus* strains (Fig. 4b; Additional File 1, Fig. S1). To exclude the errors introduced by genome sequencing or assembly, the fragment between *fenE* and *dacC* was cloned and sequenced, it was confirmed that *fenC* and *fenD* were lost in strain NCD-2 (Fig. 5a-d). To identify the enzymes FenC and FenD in the NCD-2 genome, their amino acid sequences from FZB42 were selected to screen for homologs by scanning the local NCD-2 proteome using BioEdit. The Gms1961 protein in the NCD-2 strain had the greatest similarity to FenC at an amino acid sequence level (Additional File 1, Table S2). The Gms1961 protein contained 2,550 amino acids, and the molecular weight was 287.50 kDa. The substrate bound by the adenylation domain of the Gms1961 protein was predicted (Additional File 1, Table S4). The adenylation A9 domain bound valine and N5-hydroxyornithine, with the latter being a transitional form of ornithine combined with the adenylation domain [55]. The UHPLC-QTOF MS/MS of the fengycins revealed that all the structures possessed the amino acid ornithine at position 2 (Fig. 7a-e), indicating that there was a protein that transports ornithine in the NCD-2 strain. Thus, it was hypothesized that Gms1961 functions as FenC and FenE. The same analysis was performed using the Gms1960 protein and it had the greatest similarity with FenD (Additional File 1, Table S3); however, the FenD domains in Gms1960 and FZB42 varied greatly. Therefore, it was hypothesized that Gms1960 or other enzymes may have function similar to those of FenD.

Although the fengycin biosynthetic gene cluster in the NCD-2 strain lacked two important genes-*fenC* and *fenD* compared with the reported fengycin biosynthetic gene cluster, the NCD-2 strain was capable of producing 26 homologs of 5 kinds of fengycins. The amino acids at position 6 and 10 of the fengycin cyclic peptide ring determine the type of fengycin. There are currently five types of reported fengycins, A, B, A2, B2, and C (Additional File 1, Fig. S4). When the amino acid at position 6 was valine and at position 10 was isoleucine or valine, then fengycin B or fengycin B2, respectively, was produced (Fig. 7a, b) and (Additional File 1, Fig. S4); however, if the amino acid at position 6 was alanine, then fengycin A or fengycin A2, respectively, was produced (Fig. 7c, d) and (Additional File 1, Fig. S4). When the amino acid at position 6 was isoleucine or leucine and at position 10 was valine, then fengycin C was produced (Fig. 7e) and (Additional File 1, Fig. S4). The MS analysis of the fengycins in the NCD-2 strain revealed that the strain was capable of producing these five kinds of fengycins. Based on differences in the number of carbon atoms in the  $\beta$ -OH FA, fengycin had different homologs, and the molecular weight of each homologs differed by 14 (-CH<sub>2</sub>) [56]. The molecular structure of the lipopeptide determines its biological activity, and long-chain fatty acids increase the hydrophobic activities of lipopeptides, making them more likely to have membrane-bound

Loading [MathJax]/jax/output/CommonHTML/jax.js in produces four fengycin homologs, but only fengycins with C16 and C17 carbon

atoms in their  $\beta$ -OH FA chains had antibacterial activities [58]. The NCD-2 strain produced 14 fengycin homologs having more than 16 carbon atoms, and they accounted for a large proportion of all the homologs. It was speculated that these long-chain fengycins played important roles in the antimicrobial functions of NCD-2. The *B. siamensis* SCSIO 05746 strain produces a great number of fengycin homologs, including 19 homologs of fengycin B [59]. Using MS/MS analysis, the five fengycins produced by the NCD-2 strain were divided into 26 homologs (Fig. 7a–e) and (Additional File 1, Fig. S5-S9). Therefore, NCD-2 is currently the strain with the largest number of known fengycin homologs [60].

During the microbial synthesis of secondary metabolites, such as lipopeptide, the relatively high energy-consuming process of protein synthesis takes priority [61]. Excessive energy consumption is not conducive to the normal growth of microbes, and, generally, microbes produce antibiotics in large amounts only when encountering pathogens or other stresses [62]. We hypothesized that the key biosynthetic genes *fenEAB* involved in synthesizing fengycin were conserved, while two important biosynthetic genes *fenCD* were lost in the long-term evolution of NCD-2. However, five fengycins were still produced. Gms1961 might played the dual roles of FenC and FenE, indicating that NCD-2's fengycin biosynthetic process was unique to the strain, and was more energy-efficient than the process used in the other strains..

## Conclusions

In this study, genome mining and UHPLC–QTOF–MS/MS were performed. It was found that there were many gene clusters encoding antimicrobial compounds in the genome of the NCD-2 strain and that the fengycin biosynthetic gene cluster might be unique. The results indicated that the NCD-2 strain might have a unique mechanism for synthesizing fengycin. Using bioinformatics and biochemistry to analyze the new mechanism of fengycin synthesis may provide a new theory for the synthesis of antimicrobial compounds through the NRPS pathway.

## Methods

### Microorganisms and culture conditions

*B. subtilis* NCD-2 was routinely grown at 37 °C on Luria Bertani medium. For lipopeptide, bacillaene, bacilysin, bacillibactin and subtilosin production, strain NCD-2 was grown in Landy broth [63], PA medium [64], MSA medium [65], and TSB medium [66] at 30 °C and 180 rpm. Phytopathogen *Botrytis cinerea* BC-10 was used for antifungal activity test following the method described by Guo et al [29] with some modifications. Briefly, a 6-mm diameter disc of *B. cinerea* was placed in the center of a 9-cm potato dextrose agar (PDA) plate, and the plates were inoculated with *B. subtilis* NCD-2 using a sterilized toothpick 2 cm from the center. Finally, the diameter of the inhibition zone was measured after a 3-d incubation at 25°C.

### Genome sequencing of strain NCD-2

The Illumina Solexa platform was used for the whole-genome sequencing following the method described by Karim [67] with some modifications. The quality of reads was checked using FastQC (<http://www.bioinformatics.babraham.ac.uk/projects/fastqc/>) [68], paired-end reads were trimmed using Sickle (<https://github.com/najoshi/sickle>), and were assembled using the software Velvet [30]. QUAST 5.02 was used to assess the quality of contigs and scaffolds [69]. The assembled scaffolds were annotated using Prokka (version v.1.13) [70]. The annotation of strain NCD-2 genome was performed using the NCBI Prokaryotic Genomes Automatic Annotation Pipeline ([http://www.ncbi.nlm.nih.gov/genome/annotation\\_prok/](http://www.ncbi.nlm.nih.gov/genome/annotation_prok/)) utilizing GeneMark, Glimmer, and tRNAscan-SE tools [71], and the functional annotation was carried out using the Rapid Annotations by subsystems Technology (RAST) server with the seed database [72]. Finally, the genome of strain NCD-2 was deposited in the National Center for Biotechnology Information (NCBI; <https://www.ncbi.nlm.nih.gov/>), and the GenBank accession number is CP023755.

### Evolutionary analysis, signal peptide and CRISPR repeat detection

The whole-genome sequences of *B. subtilis* and closely related species were downloaded from the NCBI database, and the Loading [MathJax]/jax/output/CommonHTML/jax.js [73] was used for genome-wide comparisons with default parameters. A

phylogenetic analysis was conducted using MEGA5 [74] with the Maximum Composite Likelihood parameter model [75]. A phylogenetic tree was constructed using the Neighbor-joining algorithm method with bootstrap values based on 1,000 replications. The signal peptide was predicted using the SignalP-5.0 website ([www.cbs.dtu.dk/services/SignalP-5.0/](http://www.cbs.dtu.dk/services/SignalP-5.0/)) [76]. CRISPR repeats were detected using CRISPRCasFinder (<https://crisprcas.i2bc.paris-saclay.fr/CrisprCasFinder/Index>) [77].

### Predictions and a specificity analysis of secondary metabolite biosynthetic gene clusters

Secondary metabolite biosynthetic gene clusters for strain NCD-2 were detected using antiSMASH (<http://antismash.secondarymetabolites.org>) [32, 78] and PRISM (<http://grid.adapsyn.com/prism/>) [79] with the parameters selected by default. Functional domain predictions for PKS/NRPS in the predicted gene clusters were analyzed using the PKS/NRPS Analysis Website (<http://nrps.igs.umaryland.edu/>) [80]. Typical PKS and NRPS sequences were selected for genomic and proteomic scanning after using BioEdit software to create a local BLAST based on strain NCD-2's genome and proteome, respectively.

### Detection of FenC and FenD lost in strain NCD-2 genome

FenC and FenD are two important enzymes for synthesizing fengycin. A pair of degenerate primers targeting the *fenE* (5'-TCATR T T GRAGMAC $\nabla$ ACAT-3) and *dacC* (5'-TGACAG $\nabla$ TGRYGGGMGG $\nabla$ C-3) were designed based on the conserved bases of *fenE* and *dacC* in strain NCD-2 and *B. velezensis* strain FZB42. 16S rDNA (27-F/1492R) primers were used as positive control [81]. The amplification procedure included a denaturation step at 95 °C for 2 min, followed by 32 cycles of 20 sec strand separation at 95 °C, 20 sec annealing at 55 °C, and 90 sec elongation at 72 °C, followed by an elongation step of 5 min at 72 °C. The target fragment from NCD-2 was purification by gel extraction kit (Sangon, Shanghai, China) and ligated to Blunt-ended vector (Transgen, Beijing, China) and sequenced by BGI company (Shenzhen, China).

### Separation of lipopeptides by FPLC

Lipopeptides were extracted using the method described by Guo et al [29]. Briefly, strain NCD-2 or derived strains were cultured in 100 mL Landy broth [63] at 30 °C for 72 h with shaking at 180 rpm. The cell-free supernatant was obtained by centrifugation at 8,000 $\times$ g for 30 min at 4 °C. The supernatant was adjusted to pH 2.0 with 6 mol/L HCl and stored for 12h at 4 °C. After centrifugation at 10,000  $\times$ g, for 20 min, the resulting pellet was extracted with 10 mL methanol under continuous magnetic stirring for 2 h. The obtained extracts were sterilized by passing through 0.45- $\mu$ m filters (Millex-GV, Millipore, Billerica, MA, USA) to obtain crude lipopeptides. The crude lipopeptides were separated and purified using an AKTA Purifier (GE Healthcare, Uppsala, Sweden) with the SOURCE 5RPC ST 4.6/150 column as described previously [82]. The lipopeptides were eluted by solvent A [2% acetonitrile containing 0.065% trifluoroacetic acid (TFA) (V/V)] and solvent B [80% acetonitrile containing 0.05% TFA (V/V)] using a linear gradient of 0%–100% acetonitrile over 57 min at a flow rate of 1 mL/min. The detection wavelength was 215 nm. All the main peaks were collected by FPLC automatically. Finally, each peak was concentrated using a rotary evaporator and was analyzed using UHPLC-QTOF–MS/MS.

### UHPLC–QTOF–MS/MS

The UHPLC–QTOF–MS/MS analysis was conducted on a hybrid quadrupole time-of-flight tandem mass spectrometer (AB SCIEX TripleTOF 5600 Q-TOF/MS, Foster City, CA, USA) with an HPLC (Shimadzu, Kyoto, Japan) that was equipped with LC-30AD binary pumps, a SIL-30AC autosampler, and a CTO-30AC column oven. A C18 reversed phase LC column (Shim-pack GIST 2- $\mu$ m particles, 2.1 mm $\times$ 100 mm) was used for separation. The mobile phases A and B were water and acetonitrile with 0.1% formic acid, respectively, in both phases with an optimized linear gradient eluting procedure, as follows: 0.0–0.5 min, 30% B; 0.5–50 min, 60% B; 50–52 min, 95% B; 52–55 min, 95% B; 55–55.1 min, 30% B; 55.1–60 min, 30% B. The injection volume was 20  $\mu$ L with a flow rate of 0.30 mL/min. The column oven was set at 40°C. The MS analysis was performed using a 5600 TripleTOF system equipped with a DuoSpray<sup>TM</sup> Ion Source, and the data were processed using Analyst TF 1.7 software (Applied Biosystems Sciex, Toronto, ON, Canada). PeakView<sup>TM</sup> software 2.0 (Applied Biosystems Sciex, Toronto, ON, Canada) was used for investigating and interpreting mass spectral data with special tools for processing accurate mass data and

Loading [MathJax]/jax/output/CommonHTML/jax.js source was used in positive ion mode. The instrumental parameters were set as

follows: ion spray voltage floating, 5,000 V; nebulizing gas, 50 psi; heater gas, 50 psi; curtain gas, 35 psi; temperature, 350°C; declustering potential (in TOF MS experiments, 100 V; and collision energy, 10.0 V. During the TOF-MS/MS declustering potential, the collision energy spread was between 100 V and 5 V, with rolling collision energy. The MS was operated in full-scan TOF-MS ( $m/z$  200–2,000) and MS/MS ( $m/z$  50–1,600) modes using Information Dependent Acquisition for a single run analysis.

### **Detection of bacillaene, bacilysin, bacillibactin and subtilisin**

For bacillaene, strain NCD-2 was cultured in 100 mL Landy broth at 30°C for 72 h with shaking at 180 rpm, and the bacillaene was extracted by methanol using the method described by Reddick et al [83]. For bacilysin, strain NCD-2 was cultured in 100 mL PA medium at 30°C for 72 h with shaking at 180 rpm, and the bacilysin was extracted by ice-cold ethanol as described by Wu et al [64]. For bacillibactin, strain NCD-2 was cultured in 100 mL MSA medium at 30°C for 72 h, and the bacillibactin was extracted by ethanol as described by Li et al [65]. For subtilisin, strain NCD-2 was cultured in 100 mL TSB medium at 30°C for 72 h, and the subtilisin was extracted by precipitation with 65% ammonium sulphate as described by Charles et al [66]. The extracts were detected by UHPLC-QTOF-MS/MS as described as above.

## **Declarations**

### **Availability of data and materials**

The datasets used and analysed during the current study are available from the corresponding author on reasonable request.

### **Abbreviations**

UHPLC-QTOF-MS/MS: ultra-high-performance liquid chromatography coupled to quadrupole-time-of-flight tandem mass spectrometry; A domain: adenylation domain; C domain :condensation domain; T domain: thiolation domain; Te: thioesterase domain; E domain: epimerization domain; N90: the minimum contig length to cover 90 percent of the genome; PDA: potato dextrose agar; BGC: biosynthetic gene cluster; FPLC: Fast protein liquid chromatography;  $m/z$ : mass-to-charge ratio; TFA: trifluoroacetic acid.  $\beta$ -OHFA:  $\beta$ -hydroxy-fatty acid.

### **Acknowledgements**

We would like to thank professor Liqun Zhang from China Agricultural University whose comments and suggestions greatly improved the quality of this article.

### **Authors' contributions**

ZHS, QGG, and PM designed the experiments. ZHS, XYC, and XML performed all the experiments. ZHS and XYC analyzed the data. ZHS, QGG, and PM wrote the manuscript. All the authors reviewed the final manuscript.

### **Funding**

This work was funded by the earmarked fund for National Key R & D Projects (2017YFD0200400), the China Agriculture Research System (CARS-18-15), the Natural Science Foundation of Hebei Province (C2019301101), the National Natural Science Foundation of China (31572051 and 31601680), the PhD Fund of Hebei Academy of Agriculture and Forestry (C19R01003), and the Special Fund for Agro-scientific Research in the Public Interest, China (201503109). We thank Lesley Benyon, PhD, from Liwen Bianji, Edanz Group China (www.liwenbianji.cn/ac), for editing the English text of a draft of this manuscript.

### **Ethics approval and consent to participate**

Not applicable.

## Consent for publication

Not applicable.

## Competing interests

The authors declare that they have no competing interests.

## Author details

Institute of Plant Protection, Hebei Academy of Agricultural and Forestry Sciences, Integrated Pest Management Center of Hebei Province, Key Laboratory of IPM on Crops in Northern Region of North China, Ministry of Agriculture, Baoding 071000, China

## References

1. Sonenshein AL. Control of sporulation initiation in *Bacillus subtilis*. *Current Opinion in Microbiology*. 2000;3(6):561-566.
2. Wang P, Guo Q, Ma Y, Li S, Lu X, Zhang X, Ma P. DegQ regulates the production of fengycins and biofilm formation of the biocontrol agent *Bacillus subtilis* NCD-2. *Microbiological Research*. 2015;178:42-50.
3. Fan H, Ru J, Zhang Y, Wang Q, Li Y. Fengycin produced by *Bacillus subtilis* 9407 plays a major role in the biocontrol of apple ring rot disease. *Microbiological Research*. 2017;199:89-97.
4. Wu Y, Wang Y, Zou H, Wang B, Sun Q, Fu A, Wang Y, Wang Y, Xu X, Li W. *Bacillus amyloliquefaciens* probiotic SC06 induces autophagy to protect against pathogens in macrophages. *Frontiers in Microbiology*. 2017;8:469.
5. Moszer I, Jones L, Moreira S, Fabry C, Danchin A. SubtiList: the reference database for the *Bacillus subtilis* genome. *Nucleic Acids Research*. 2002;30(1):62-65.
6. Torres MJ, Brandan CP, Sabate DC, Petroselli G, Errabalsells R, Audisio MC. Biological activity of the lipopeptide-producing *Bacillus amyloliquefaciens* PGPBacCA1 on common bean *Phaseolus vulgaris* L. pathogens. *Biological Control*. 2017;105:93-99.
7. Agustín L-B, Raunel T-V, Gerardo C, Kohei K, Katsuhiko K, Enrique G, Leobardo S-C. Effects of bacillomycin D homologues produced by *Bacillus amyloliquefaciens* 83 on growth and viability of *Colletotrichum gloeosporioides* at different physiological stages. *Biological Control*. 2018;127:145-154.
8. Stein T. *Bacillus subtilis* antibiotics: structures, syntheses and specific functions. *Molecular Microbiology*. 2005;56(4):845-857.
9. Beppu T. Secondary metabolites as chemical signals for cellular differentiation. *Gene*. 1992;115(1-2):159-165.
10. Chaudhary AK, Dhakal D, Sohng JK. An insight into the "-omics" based engineering of streptomycetes for secondary metabolite overproduction. *BioMed Research International*. 2013;2013:968518-968518.
11. Kröber M, Wibberg D, Grosch R, Eikmeyer F, Verwaaijen B, Chowdhury SP, Hartmann A, Pühler A, Schlüter A. Effect of the strain *Bacillus amyloliquefaciens* FZB42 on the microbial community in the rhizosphere of lettuce under field conditions analyzed by whole metagenome sequencing. *Frontiers in Microbiology*. 2014;5:252-252.
12. Ichikawa N, Sasagawa M, Yamamoto M, Komaki H, Yoshida Y, Yamazaki S, Fujita N. DoBISCUIT: a database of secondary metabolite biosynthetic gene clusters. *Nucleic Acids Research*. 2012;41(D1):D408-D414.
13. Chen XH, Koumoutsis A, Scholz R, Borriss R. More than anticipated - production of antibiotics and other secondary metabolites by *Bacillus amyloliquefaciens* FZB42. *Journal of Molecular Microbiology and Biotechnology*. 2009;16(1-2):14-24.
14. Stein T, Vater J, Kruff V, Otto A, Wittmannliebhold B, Franke P, Panico M, McDowell RA, Morris HR. The multiple carrier model of nonribosomal peptide biosynthesis at modular multienzymatic templates. *Journal of Biological Chemistry*. 1996;271(26):15428-15435.

16. Arguellesarias A, Ongena M, Halimi B, Lara Y, Brans A, Joris B, Fickers P. *Bacillus amyloliquefaciens* GA1 as a source of potent antibiotics and other secondary metabolites for biocontrol of plant pathogens. *Microbial Cell Factories*. 2009;8(1):63-63.
17. Tamehiro N, Okamotohosoya Y, Okamoto S, Ubukata M, Hamada M, Naganawa H, Ochi K. Bacilysocin, a novel phospholipid antibiotic produced by *Bacillus subtilis* 168. *Antimicrobial Agents and Chemotherapy*. 2002;46(2):315-320.
18. Carrillo C, Teruel JA, Aranda FJ, Ortiz A. Molecular mechanism of membrane permeabilization by the peptide antibiotic surfactin. *Biochimica et Biophysica Acta*. 2003;1611(1-2):91-97.
19. Yu GY, Sinclair JB, Hartman GL, Bertagnolli BL. Production of iturin A by *Bacillus amyloliquefaciens* suppressing *Rhizoctonia solani*. *Soil Biology & Biochemistry*. 2002;34(7):955-963.
20. Jacques P, Hbid C, Destain J, Razafindralambo H, Paquot M, De Pauw E, Thonart P. Optimization of biosurfactant lipopeptide production from *Bacillus subtilis* S499 by plackett-burman design. *Applied Biochemistry and Biotechnology*. 1999;77-79:223-233.
21. Moyne A, Cleveland TE, Tuzun S. Molecular characterization and analysis of the operon encoding the antifungal lipopeptide bacillomycin D. *FEMS Microbiology Letters*. 2004;234(1):43-49.
22. Tulp M, Bohlin L. Rediscovery of known natural compounds: nuisance or goldmine? *Bioorganic & Medicinal Chemistry*. 2005;13(17):5274-5282.
23. von Bubnoff A. Seeking new antibiotics in nature's backyard. *Cell*. 2006;127(5):867-869.
24. Oman TJ, van der Donk WA. Follow the leader: the use of leader peptides to guide natural product biosynthesis. *Nature Chemical Biology*. 2010;6(1):9-18.
25. Lane AL, Moore BS. A sea of biosynthesis: marine natural products meet the molecular age. *Natural Product Reports*. 2011;28(2):411-428.
26. Rutledge PJ, Challis GL. Discovery of microbial natural products by activation of silent biosynthetic gene clusters. *Nature Reviews Microbiology*. 2015;13(8):509-523.
27. van Dijk EL, Auger H, Jaszczyszyn Y, Thermes C. Ten years of next-generation sequencing technology. *Trends in genetics*. 2014;30(9):418-426.
28. Guo Q, Li S, Lu X, Li B, Ma P. PhoR/PhoP two component regulatory system affects biocontrol capability of *Bacillus subtilis* NCD-2. *Genetics and Molecular Biology*. 2010;33(2):333-340.
29. Guo Q, Dong W, Li S, Lu X, Wang P, Zhang X, Wang Y, Ma P. Fengycin produced by *Bacillus subtilis* NCD-2 plays a major role in biocontrol of cotton seedling damping-off disease. *Microbiological Research*. 2014;169(7-8):533-540.
30. Zerbino D, Birney E. Velvet : algorithms for *de novo* short read assembly using de bruijn graphs. *Genome Research*. 2008;18(5):821-829.
31. Dunlap CA, Bowman MJ, Zeigler DR. Promotion of *Bacillus subtilis* subsp. *inaquosorum*, *Bacillus subtilis* subsp. *spizizenii* and *Bacillus subtilis* subsp. *stercoris* to species status. *Antonie Van Leeuwenhoek International Journal of General and Molecular Microbiology*. 2020;113(1):1-12.
32. Blin K, Medema MH, Kazempour D, Fischbach MA, Breitling R, Takano E, Weber T. antiSMASH 2.0—a versatile platform for genome mining of secondary metabolite producers. *Nucleic Acids Research*. 2013;41(W1):W204-W212.
33. Sansinenea E, Ortiz A. Secondary metabolites of soil *Bacillus* spp. *Biotechnology Letters*. 2011;33(8):1523-1538.
34. Yu D, Fang Y, Tang C, Klosterman SJ, Tian C, Wang Y. Genomewide transcriptome profiles reveal how *Bacillus subtilis* lipopeptides inhibit microsclerotia formation in *Verticillium dahliae*. *Molecular Plant-microbe Interactions*. 2019;32(5):622-634.
35. Xiao X, Chen H, Chen H, Wang J, Ren C, Wu L. Impact of *Bacillus subtilis* JA, a biocontrol strain of fungal plant pathogens, on arbuscular mycorrhiza formation in *Zea mays*. *World Journal of Microbiology & Biotechnology*. 2008;24(7):1133-1137.
36. Challis GL, Ravel J. Coelichelin, a new peptide siderophore encoded by the *Streptomyces coelicolor* genome: structure prediction from the sequence of its non-ribosomal peptide synthetase. *FEMS Microbiology Letters*. 2000;187(2):111-114.

37. Basichipalu S, Dischinger J, Josten M, Szekat C, Zweynert A, Sahl H, Bierbaum G. Pseudomycoicidin, a class II lantibiotic from *Bacillus pseudomycooides*. Applied and Environmental Microbiology. 2015;81(10):3419-3429.
38. Seydlová G, Svobodová J. Review of surfactin chemical properties and the potential biomedical applications. Central European Journal of Medicine. 2008;3(2):123-133.
39. Patel PS, Huang S, Fisher S, Pirnik D, Aklonis C, Dean L, Meyers E, Fernandes P, Mayerl F. Bacillaene, a novel inhibitor of procaryotic protein synthesis produced by *Bacillus subtilis*. Journal of Antibiotics. 2006;48(9):997.
40. Ramarathnam R, Bo S, Chen Y, Fernando WG, Xuewen G, de Kievit T. Molecular and biochemical detection of fengycin- and bacillomycin D-producing *Bacillus* spp., antagonistic to fungal pathogens of canola and wheat. Canadian Journal of Microbiology. 2007;53(7):901-911.
41. Miethke M, Klotz O, Linne U, May JJ, Beckering CL, Marahiel MA. Ferri-bacillibactin uptake and hydrolysis in *Bacillus subtilis*. Molecular Microbiology. 2006;61(6):1413-1427.
42. Thennarasu S, Lee DK, Poon A, Kawulka KE, Vederas JC, Ramamoorthy A. Membrane permeabilization, orientation, and antimicrobial mechanism of subtilosin A. Chemistry and Physics of Lipids. 2005;137(1-2):38-51.
43. Kenig M, Abraham EP. Antimicrobial activities and antagonists of bacilysin and anticapsin. Microbiology. 1976;94(1):37-45.
44. Li B, Li Q, Xu Z, Zhang N, Shen Q, Zhang R. Responses of beneficial *Bacillus amyloliquefaciens* SQR9 to different soilborne fungal pathogens through the alteration of antifungal compounds production. Frontiers in Microbiology. 2014;5:636-636.
45. Wu L, Wu H, Chen L, Yu X, Borriss R, Gao X. Difficidin and bacilysin from *Bacillus amyloliquefaciens* FZB42 have antibacterial activity against *Xanthomonas oryzae* rice pathogens. Scientific Reports. 2015;5:12975.
46. Nonejuie P, Trial RM, Newton GL, Lamsa A, Perera VR, Aguilar J, Liu W, Dorrestein PC, Pogliano J, Pogliano K. Application of bacterial cytological profiling to crude natural product extracts reveals the antibacterial arsenal of *Bacillus subtilis*. The Journal of Antibiotics. 2016;69:353-361.
47. Goodson JR, Klupt S, Zhang C, Straight PD, Winkler WC. LoaP is a broadly conserved antiterminator protein that regulates antibiotic gene clusters in *Bacillus amyloliquefaciens*. Nature Microbiology. 2017;2(5):1-10.
48. Fan B, Wang C, Song X, Ding X, Wu L, Wu H, Gao X, Borriss R. *Bacillus velezensis* FZB42 in 2018: The gram-positive model strain for plant growth promotion and biocontrol. Frontiers in Microbiology. 2018;9:2491.
49. Jin P, Wang H, Liu W, Miao W. Characterization of *lpaH2* gene corresponding to lipopeptide synthesis in *Bacillus amyloliquefaciens* HAB-2. BMC Microbiology. 2017;17(1):227.
50. Chen X, Koumoutsis A, Scholz R, Eisenreich A, Schneider K, Heinemeyer I, Morgenstern B, Voss B, Hess W, Reva O *et al.* Comparative analysis of the complete genome sequence of the plant growth-promoting bacterium *Bacillus amyloliquefaciens* FZB42. Nature Biotechnology. 2007;25(9):1007-1014.
51. Koumoutsis A, Chen X, Henne A, Liesegang H, Hitzeroth G, Franke P, Vater J, Borriss R. Structural and functional characterization of gene clusters directing nonribosomal synthesis of bioactive cyclic lipopeptides in *Bacillus amyloliquefaciens* strain FZB42. Journal of Bacteriology. 2004;186(4):1084-1096.
52. Chen C, Chang L, Chang Y, Liu S, Tschen JS. Transposon mutagenesis and cloning of the genes encoding the enzymes of fengycin biosynthesis in *Bacillus subtilis*. Molecular Genetics and Genomics. 1995;248(2):121-125.
53. Lin G, Chen C, Tschen JS, Tsay S, Chang Y, Liu S. Molecular cloning and characterization of fengycin synthetase gene *fenB* from *Bacillus subtilis*. Journal of Bacteriology. 1998;180(5):1338-1341.
54. Lin TP, Chen CL, Chang LK, Tschen JS, Liu ST. Functional and transcriptional analyses of a fengycin synthetase gene, *fenC*, from *Bacillus subtilis*. Journal of Bacteriology. 1999;181(16):5060-5067.
55. Lautru S, Deeth RJ, Bailey LM, Challis GL. Discovery of a new peptide natural product by *Streptomyces coelicolor* genome mining. Nature Chemical Biology. 2005;1(5):265-269.
56. Bie XM, Lü FX, Lu ZX, Huang XQ, Shen J. [Isolation and identification of lipopeptides produced by *Bacillus subtilis* fmbJ]. Sheng wu gong cheng xue bao = Chinese journal of biotechnology. 2006;22(4):644-649.

57. Tripathi L, Irerere VU, Marchant R, Banat IM. Marine derived biosurfactants: a vast potential future resource. *Biotechnology Letters*. 2018;40(11-12):1441-1457.
58. Sivapathasekaran C, Mukherjee S, Samanta R, Sen R. High-performance liquid chromatography purification of biosurfactant isoforms produced by a marine bacterium. *Analytical and Bioanalytical Chemistry*. 2009;395(3):845-854.
59. Pan H, Tian X, Shao M, Xie Y, Huang H, Hu J, Ju J. Genome mining and metabolic profiling illuminate the chemistry driving diverse biological activities of *Bacillus siamensis* SCSIO 05746. *Applied Microbiology and Biotechnology*. 2019;103(10):4153-4165.
60. Ongena M, Jacques P. *Bacillus lipopeptides*: versatile weapons for plant disease biocontrol. *Trends in Microbiology*. 2008;16(3):115-125.
61. Bhat A, Chakraborty R, Adlakha K, Agam G, Chakraborty K, Sengupta S. Ncl1-mediated metabolic rewiring critical during metabolic stress. *Life Science Alliance*. 2019;2(4).
62. Bae J, Park J, Hahn M, Kim M, Roe J. Redox-dependent changes in RsrA, an anti-sigma factor in *Streptomyces coelicolor*. Zinc release and disulfide bond formation. *Journal of Molecular Biology*. 2004;335(2):425-435.
63. Landy M, Warren GH. Bacillomycin; an antibiotic from *Bacillus subtilis* active against pathogenic fungi. *Proceedings of the Society for Experimental Biology and Medicine Society for Experimental Biology and Medicine (New York, NY)*. 1948;67(4):539-541.
64. Wu L, Wu H, Chen L, Xie S, Zang H, Borriss R, Gao X. Bacilysin from *Bacillus amyloliquefaciens* FZB42 has specific bactericidal activity against harmful algal bloom species. *Applied and Environmental Microbiology*. 2014;80(24):7512-7520.
65. Li Y, Jiang W, Gao R, Cai Y, Guan Z, Liao X. Fe(III)-based immobilized metal-affinity chromatography (IMAC) method for the separation of the catechol siderophore from CD36. *3 Biotech*. 2018;8(9):392.
66. Shelburne C, An F, Dholpe V, Ramamoorthy A, Lopatin D, Lantz M. The spectrum of antimicrobial activity of the bacteriocin subtilosin A. *The Journal of Antimicrobial Chemotherapy*. 2007;59(2):297-300.
67. Karim A, Poirot O, Khatoon A, Aurongzeb M. Draft genome sequence of a novel *Bacillus glycinifermentans* strain having antifungal and antibacterial properties. *Journal of Global Antimicrobial Resistance*. 2019;19:308-310.
68. Andrews S. FastQC A quality control tool for high throughput sequence data. 2010.
69. Alexey G, Vladislav S, Nikolay V, Glenn T: QUASt: quality assessment tool for genome assemblies. In: *2013*, 2013: 1072-1075.
70. Torsten S. Prokka: rapid prokaryotic genome annotation. *Bioinformatics*. 2014;30(14):2068-2069.
71. Disz T, Akhter S, Cuevas DA, Olson R, Overbeek R, Vonstein V, Stevens R, Edwards R. Accessing the SEED genome databases via web services API: tools for programmers. *BMC Bioinformatics*. 2010;11(1):319-319.
72. Aziz RK, Bartels D, Best AA, Dejongh M, Disz T, Edwards R, Formsma K, Gerdes S, Glass EM, Kubal M. The rast server: rapid annotations using subsystems technology. *BMC Genomics*. 2008;9:75.
73. Haubold B, Klotzl F, Pfaffelhuber P. andi: fast and accurate estimation of evolutionary distances between closely related genomes. *Bioinformatics*. 2015;31(8):1169-1175.
74. Tamura K, Peterson DS, Peterson N, Stecher G, Nei M, Kumar S. MEGA5: molecular evolutionary genetics analysis using maximum likelihood, evolutionary distance, and maximum parsimony methods. *Molecular Biology and Evolution*. 2011;28(10):2731-2739.
75. Xu X, Reid N. On the robustness of maximum composite likelihood estimate. *Journal of Statistical Planning and Inference*. 2011;141(9):3047-3054.
76. Armenteros JJA, Tsirigos KD, Sønderby CK, Petersen TN, Winther O, Brunak S, Nielsen H. SignalP 5.0 improves signal peptide predictions using deep neural networks. *Nature Biotechnology*. 2019;37(4):420-423.
77. Couvin D, Bernheim A, Toffano-Nioche C, Touchon M, Michalik J, Néron B, Rocha EPC, Vergnaud G, Gautheret D, Pourcel C. CRISPRCasFinder, an update of CRISPRFinder, includes a portable version, enhanced performance and integrates search for

78. Medema MH, Blin K, Cimermancic P, De Jager V, Zakrzewski P, Fischbach MA, Weber T, Takano E, Breitling R. antiSMASH: rapid identification, annotation and analysis of secondary metabolite biosynthesis gene clusters in bacterial and fungal genome sequences. *Nucleic Acids Research*. 2011;39(2):W339-W346.
79. Skinnider MA, Dejong CA, Rees PN, Johnston CW, Li H, Webster ALH, Wyatt MA, Magarvey NA. Genomes to natural products PRediction Informatics for Secondary Metabolomes (PRISM). *Nucleic Acids Research*. 2015;43(20):9645-9662.
80. Bachmann BO, Ravel J. Methods for in silico prediction of microbial polyketide and nonribosomal peptide biosynthetic pathways from DNA sequence data. *Methods in Enzymology*. 2009;458:181-217.
81. Byers H, Stackebrandt E, Hayward C, Blackall LL. Molecular investigation of a microbial mat associated with the Great Artesian Basin. *FEMS Microbiology Ecology*. 1998;25(4):391-403.
82. Li B, Lu X, Guo Q, Qian C, Li S, Ma P. Isolation and identification of lipopeptides and volatile compounds produced by *Bacillus subtilis* strain BAB-1, vol. 43; 2010.
83. Reddick J, Antolak S, Raner G. PksS from *Bacillus subtilis* is a cytochrome P450 involved in bacillaene metabolism. *Biochemical and Biophysical Research Communications*. 2007;358(1):363-367.

## Tables

**Table 1** Secondary metabolite gene clusters annotated in *B. subtilis* NCD-2 using antiSMASH

Cluster	Type	From	To	Most similar known cluster	Similarity	MIBiG BGC-ID*
cluster 1	NRPS	347853	413245	surfactin	82%	BGC0000433_c1
cluster 2	Terpene	1137768	1158574	-	-	-
cluster 3	NRPS-TransAT PKS-Other KS	1763940	1873766	bacillaene	100%	BGC0001089_c1
cluster 4	NRPS	1936035	2004508	fengycin	93%	BGC0001095_c1
cluster 5	Terpene	2060609	208250	-	-	-
cluster 6	T3PKS	2261562	2302659	-	-	-
cluster 7	NRPS	3225454	3275189	bacillibactin	100%	BGC0000309_c1
cluster 8	Sactipeptide-head to tail	3817363	3838974	subtilosin	100%	BGC0000602_c1
cluster 9	Other	3842273	3883691	bacilysin	100%	BGC0001184_c1

\*Identification numbers of the most similar gene clusters from *B. velezensis* FZB42 provided by the MIBiG BGC database. NRPS, non-ribosomal peptide synthetase; PKS, polyketide synthase; T3PKS, type III polyketide; NRPS-TransAT PKS-Other KS, non-ribosomal peptide synthetase-trans-AT polyketide synthase-Other types of polyketide synthase cluster; Sactipeptide-head to tail, head-to-tail cyclised peptide.

**Table 2** Fengycin homologs in NCD-2 based on key product ions of  $\beta$ -OH-FA with different chain lengths.

fengycin family	$[M+2H]^{2+}$	$\beta$ -hydroxy fatty acid
fengycin A	718.4, 725.4, 732.4, 739.4, 745.4, 753.4	C14-C19
fengycin B	718.4, 725.4, 732.4, 739.4, 746.4, 753.4, 760.4, 767.4	C12-C19
fengycin A2	718.4, 725.4, 732.4, 739.4	C15-C18
fengycin B2	725.4, 732.4, 739.4, 746.4, 753.4	C14-C18
fengycin C	760.4, 767.4, 774.5	C18-C20

## Additional Files

### Additional file 1: Supplemental Material.

Files contain supplemental materials, including supplementary tables and figures referenced in this manuscript. Fig. S1. Fengycin biosynthetic gene clusters of different strains which have a close relative with NCD-2 or model strains. Fig. S2. Surfactin biosynthetic gene clusters of different strains which have a close relative with NCD-2 or model strains. Fig. S3. Elution of lipopeptides separated from the crude methanolic extract using an AKTA Purifier. Fig. S4. Primary structures of fengycins and surfactins. Fig. S5. Fengycin A of  $\beta$ -OH FA with the chain length varying from C14 to C19 are identified based on key product ions. Fig. S6. Fengycin B of  $\beta$ -OH FA with the chain length varying from C12 to C19 are identified based on key product ions. Fig. S7. Fengycin A2 of  $\beta$ -OH FA with the chain length varying from C15-C18 are identified based on key product ions. Fig. S8. Fengycin B2 of  $\beta$ -OH FA with the chain length varying from C14-C18 are identified based on key product ions. Fig. S9. Fengycin C of  $\beta$ -OH FA with the chain length varying from C18-C20 are identified based on key product ions. Fig. S10. Surfactin of fatty acid with the chain length varying from C11-C15 are identified based on key product ions. Table S1. All the *B. subtilis* strain with the assembly level of chromosome and their RefSeq assembly accession. Table S2. The homologues of FenC of FZB42 by scanning the local NCD-2 proteome in BioEdit. Table S3. The homologues of FenD of FZB42 by scanning the local NCD-2 proteome in BioEdit. Table S4. Adenylation domain binding amino acids predicted by PRISM.

**Supplementary Fig. S1** Fengycin BGCs of different strains which had a close relative with NCD-2 or model strains. FZB42 was belonging to *B. velezensis* and others were *B. subtilis*. Different color blocks represented genes with conserved functions, take FZB42 strain for example, the fengycin biosynthetic gene cluster included genes *fenCDEAB* (also named *ppsABCDE*) in order from right to left. In strain NCD-2, there just existed genes *fenEAB* which was specially different from other strains.

**Supplementary Fig. S2** Surfactin BGCs of different strains which had a close relative with NCD-2 or model strains. FZB42 was belonging to *B. velezensis* and others were *B. subtilis*. Different color blocks represented genes with conserved functions, take FZB42 strain for example, the surfactin biosynthetic gene cluster included genes *srfAABCD* in order from left to right. In strain NCD-2, *srfAB* was divided into two genes to transcribe and translate which was different from other strains.

**Supplementary Fig. S3** Elution of lipopeptides separated from the crude methanolic extract of *B. subtilis* NCD-2. An AKTA Purifier (GE Healthcare, Uppsala, Sweden) with the SOURCE 5RPC ST 4.6/150 column was used, the fractions (P2-P25) are shown above the peaks. Fractions 12, 13, 14, 15 were fengycins and fractions 19, 20 were surfactin.

**Supplementary Fig. S4** Primary structures of fengycins and surfactins. (a) The overall structure of Fengycins; (b) Fengycin A, fengycin B, fengycin A2, fengycin B2, and fengycin C. Sites of mass spectrometric cleavage with the  $m/z$  values for diagnostic product ions ( $\alpha$  and  $\beta$ ) were indicated; (c) the overall structure of surfactins.

**Supplementary Fig. S5** Fengycin A were identified.  $\beta$ -OH FA with the chain length varied from C14 to C19 based on key product ions ( $[M+2H]^{2+}$ : 718.4, 725.4, 732.4, 739.4, 745.4, and 753.4).

**Supplementary Fig. S6** Fengycin B were identified.  $\beta$ -OH FA with the chain length varied from C12 to C19 were identified based on key product ions ( $[M+2H]^{2+}$ : 718.4, 725.4, 732.4, 739.4, 746.4, 753.4, 760.4, and 767.4).

**Supplementary Fig. S7** Fengycin A2 were identified.  $\beta$ -OH FA with the chain length varied from C15-C18 were identified based on key product ions ( $[M+2H]^{2+}$ : 718.4, 725.4, 732.4, and 739.4).

**Supplementary Fig. S8** Fengycin B2 were identified.  $\beta$ -OH FA with the chain length varied from C14-C18 were identified based on key product ions ( $[M+2H]^{2+}$ : 725.4, 732.4, 739.4, 746.4, and 753.4).

**Supplementary Fig. S9** Fengycin C were identified.  $\beta$ -OH FA with the chain length varied from C18-C20 were identified based on key product ions ( $[M+2H]^{2+}$ : 760.4, 767.4, and 774.5).

**Supplementary Fig. S10** Surfactin were identified.  $\beta$ -OH FA with the chain length varied from C11-C15 were identified based on key product ions ( $[M+H]^+$ : 994.6, 1008.7, 1022.7 and 1036.7).

## Supplementary Tables

**Table S1** All *B. subtilis* strain with the assembly level of complete genome or chromosome and their RefSeq assembly accession.

strain	RefSeq assembly accession	strain	RefSeq assembly accession	strain	RefSeq assembly accession
168	GCF_000155325.1	SRCM103571	GCF_004103595.1	NBRC 13719	GCF_006741845.1
BEST7003	GCF_000523045.1	SRCM103576	GCF_004119615.1	RO-NN-1	GCF_000227485.1
B5n5	GCF_000186745.1	SRCM103581	GCF_004119655.1	AG1839	GCF_000699525.1
BS49Ch	GCF_000953615.1	SRCM103612	GCF_004119775.1	BAB-1	GCF_000349795.1
HJ5	GCF_000973605.1	SRCM103622	GCF_004119835.1	BSP1	GCF_000321395.1
KCTC 1028	GCF_000971925.1	SRCM103629	GCF_004119815.1	AG174	GCF_000699465.1
PY79	GCF_000497485.1	SRCM103637	GCF_004119875.1	NCIB 3610	GCF_000186085.1
QB928	GCF_000293765.1	SRCM103641	GCF_004119555.1	OH 131.1	GCF_000706705.1
50-1	GCF_003184225.1	SRCM103689	GCF_004119535.1	2KL1	GCF_003665395.1
7702	GCF_002272405.1	SRCM103696	GCF_004119595.1	2RL2-3	GCF_003665275.1
ATCC 11774	GCF_004101945.1	SRCM103697	GCF_004119635.1	3NA	GCF_000827065.1
ATCC 13952	GCF_000772125.1	SRCM103773	GCF_004119675.1	168G	GCF_001703495.1
ATCC 19217	GCF_000772165.1	SRCM103835	GCF_004119715.1	BSD-2	GCF_001465815.1
ATCC 21228	GCF_002982175.1	SRCM103837	GCF_004119695.1	CU1050	GCF_001541905.1
B-1	GCF_000769515.1	SRCM103862	GCF_004101345.1	D12-5	GCF_001596535.1
BJ3-2	GCF_002893805.1	SRCM103881	GCF_004101445.1	delta6	GCF_001660525.1
Bs-916	GCF_000772205.1	SRCM103886	GCF_004101365.1	G7	GCF_004328925.1
BS16045	GCF_001720505.1	SRCM103923	GCF_004101405.1	GFR-12	GCF_003665195.1
CW14	GCF_002163815.1	SRCM103971	GCF_004101465.1	IITK SM	GCF_003426125.1
DKU_NT_02	GCF_002269175.1	SRCM104005	GCF_004101425.1	KCTC 3135	GCF_001697265.1
DKU_NT_03	GCF_002269195.1	SRCM104008	GCF_004101485.1	MH-1	GCF_003665235.1
FDAARGOS_606	GCF_006364495.1	SRCM104011	GCF_004101565.1	N1-1	GCF_003665335.1
ge28	GCF_002202055.1	SX01705	GCF_002216085.1	N2-2	GCF_003665315.1
GS 188	GCF_002220075.1	SZMC 6179J	GCF_001604995.1	N3-1	GCF_003665355.1
H19	GCF_005234095.1	TLO3	GCF_002290305.1	N4-2	GCF_003665295.1
HJ0-6	GCF_001704095.1	TO-A JPC	GCF_001037985.1	PJ-7	GCF_003665215.1
MBI 600	GCF_005160425.1	UD1022	GCF_001015095.1	SRCM100333	GCF_002201995.1
MZK05	GCF_003612735.1	WB800N	GCF_003610955.1	SRCM100757	GCF_002173715.1
NRS 231	GCF_005153965.1	DE111	GCF_001534785.1	SRCM100761	GCF_002201955.1
PR10	GCF_005849145.1	KCTC 13429	GCF_003148415.1	SRCM101392	GCF_002202035.1
PS832	GCF_000789295.1	BEST195	GCF_000209795.2	SRCM101441	GCF_002173615.1
QB61	GCF_003148355.1	CGMCC 2108	GCF_001565875.1	SRCM101444	GCF_002173695.1
SEM-9	GCF_006165085.1	ATCC 6633	GCF_006094475.1	SSJ-1	GCF_003665255.1
SG6	GCF_000782835.1	W23	GCF_000146565.1	XF-1	GCF_000338735.1

SRCM103517	GCF_004103535.1	TU-B-10	GCF_000227465.1	NCD-2	GCF_002556525.1
SRCM103551	GCF_004103555.1	6051-HGW	GCF_000344745.1		

---

**Table S2** The homologues of FenC of FZB42 by scanning the local NCD-2 proteome in BioEdit.

protein number	score	similarity	E-value	function description
Gms1961	2701	55	0.0	FenE
Gms1960	2036	43	0.0	FenA
Gms0365	1639	37	0.0	SrfAA
Gms0366	1296	34	0.0	SrfAB
Gms3368	1127	34	0.0	DhbF
Gms1826	572	27	e-164	PKSJ
Gms1829	516	30	e-147	PKSN
Gms0367	489	39	e-138	Surfactin synthase subunit 2
Gms1959	478	30	e-135	FenB
Gms0368	462	29	e-130	SrfAC
Gms4064	234	32	6e-062	DltA

**Table S3** The homologues of FenD of FZB42 by scanning the local NCD-2 proteome in BioEdit.

protein number	score	similarity	E-value	function description
Gms1960	1719	38	0.0	FenA
Gms0365	1715	37	0.0	SrfAA
Gms1961	1706	39	0.0	FenE
Gms0366	1481	35	0.0	Surfactin synthase subunit 1
Gms3368	1179	35	0.0	DhbF
Gms1959	814	41	0.0	FenB
Gms0368	739	38	0.0	SrfAC
Gms1826	620	27	e-178	PKSJ
Gms1829	560	32	e-160	PKSN
Gms0367	519	40	e-148	Surfactin synthase subunit 2

**Table S4** Adenylation domain binding amino acids predicted by PRISM.

Gms1961	A domain A9	Val	Ile	Leu	Val	Phe	Asp	Tyr	Glu	Ala	N5-hydroxy-Orn
	score	943.0	595.0	566.0	556.5	515.2	483.3	482.8	482.7	475.2	109.9
Gms1959	A domain A13	Ile	Val	Val	Leu	Phe	Ala	Tyr	Leu	Glut	$\beta$ -Phe
	score	819.1	645.3	535.3	508.4	469.7	430.9	424.1	421.7	402.9	109.1

Predicted by PRISM (<http://grid.adapsyn.com/prism/>). The score represented the ability of adenylation domain binding amino acids.

## Figures

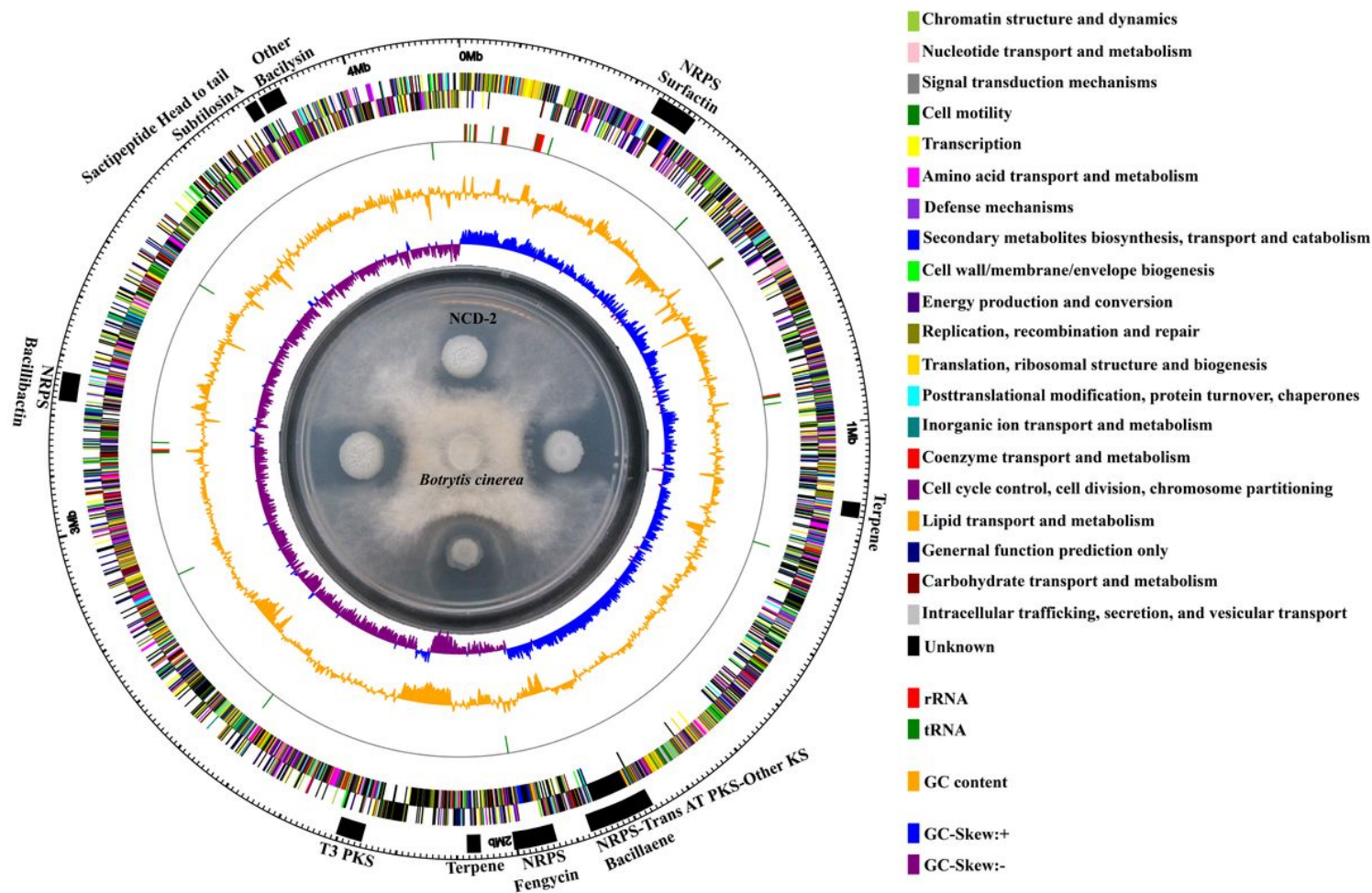


**Figure 1**

Circular genome of strain NCD-2 with specific features. The circular genome map was created using Circos v0.66 with COG (Cluster of Orthologous Groups of proteins) function annotation. From outside to inside, circle 1, the size of complete genome; circle 2 and 3, the predicted protein-coding genes on the + and - strands, different colors represent different COG function classification; circle 4, tRNA (green) and rRNA (red); circle 5, G + C content, peaks out/inside the circle indicate above or below average GC content, respectively; the inner circle, G + C skew, with  $G\% < C\%$  in purple, with  $G\% > C\%$  in blue. The potato dextrose agar plate inside the representation of the circular genome showed the antifungal activity of strain NCD-2 and its derived strain against *Botrytis cinerea*. The black bars outside the circular genome indicate the secondary metabolite biosynthetic gene clusters.

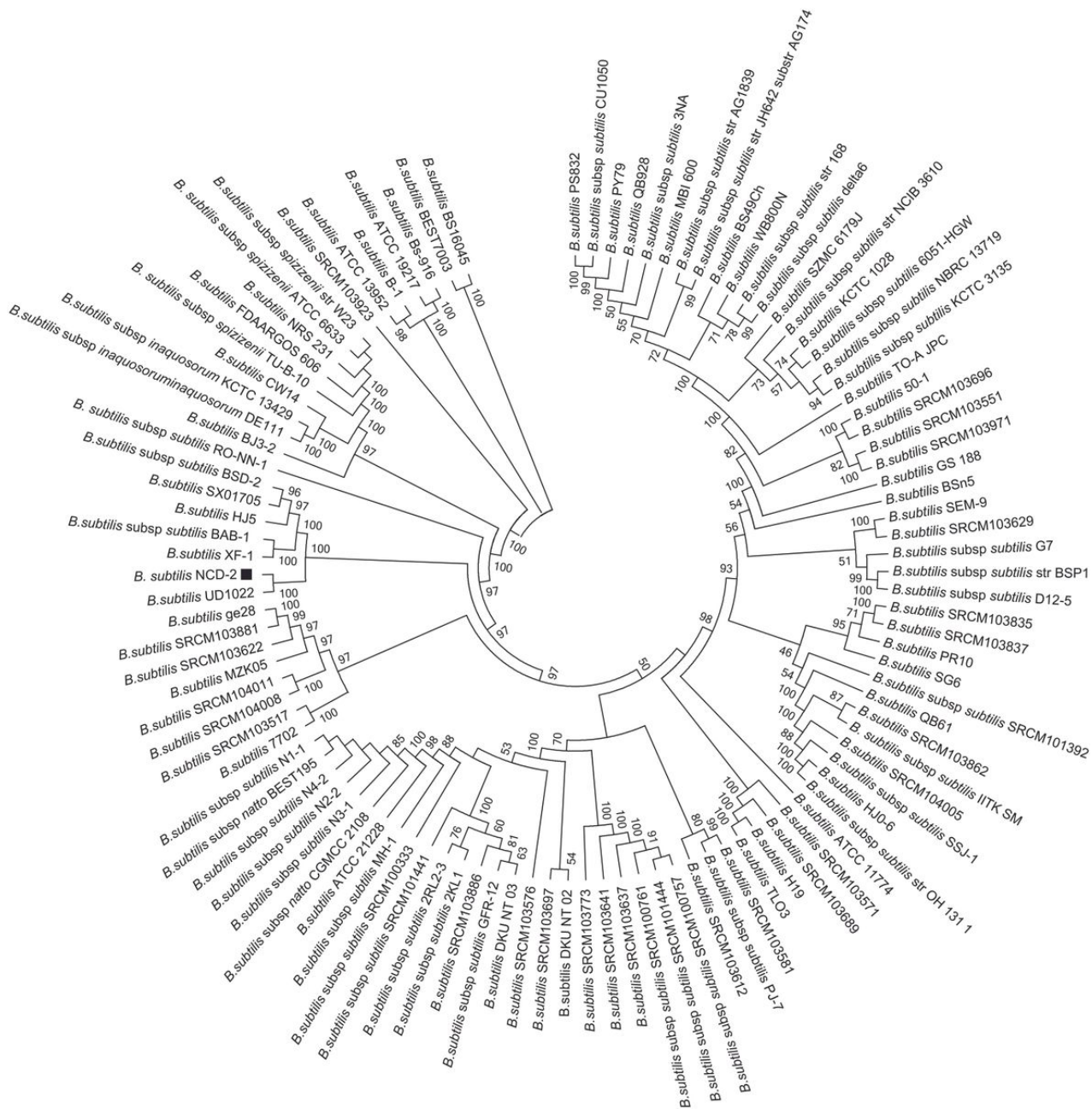


**Figure 2**

Phylogenetic tree of 113 *B. subtilis* strains based on whole genome alignments. The position of strain NCD-2 in the phylogenetic tree was indicated by a black bar. Single Nucleotide Polymorphisms (SNPs) and short insertions or deletions (indels) within the multiple sequence alignments constructed by REALPHY pipeline were extracted for subsequent phylogeny reconstruction. The phylogenetic tree was constructed using MEGA 5.0 by the Neighbor-joining method, with a bootstrap of 1,000 replications. Bootstrap confidence levels > 50% are indicated at the internodes.

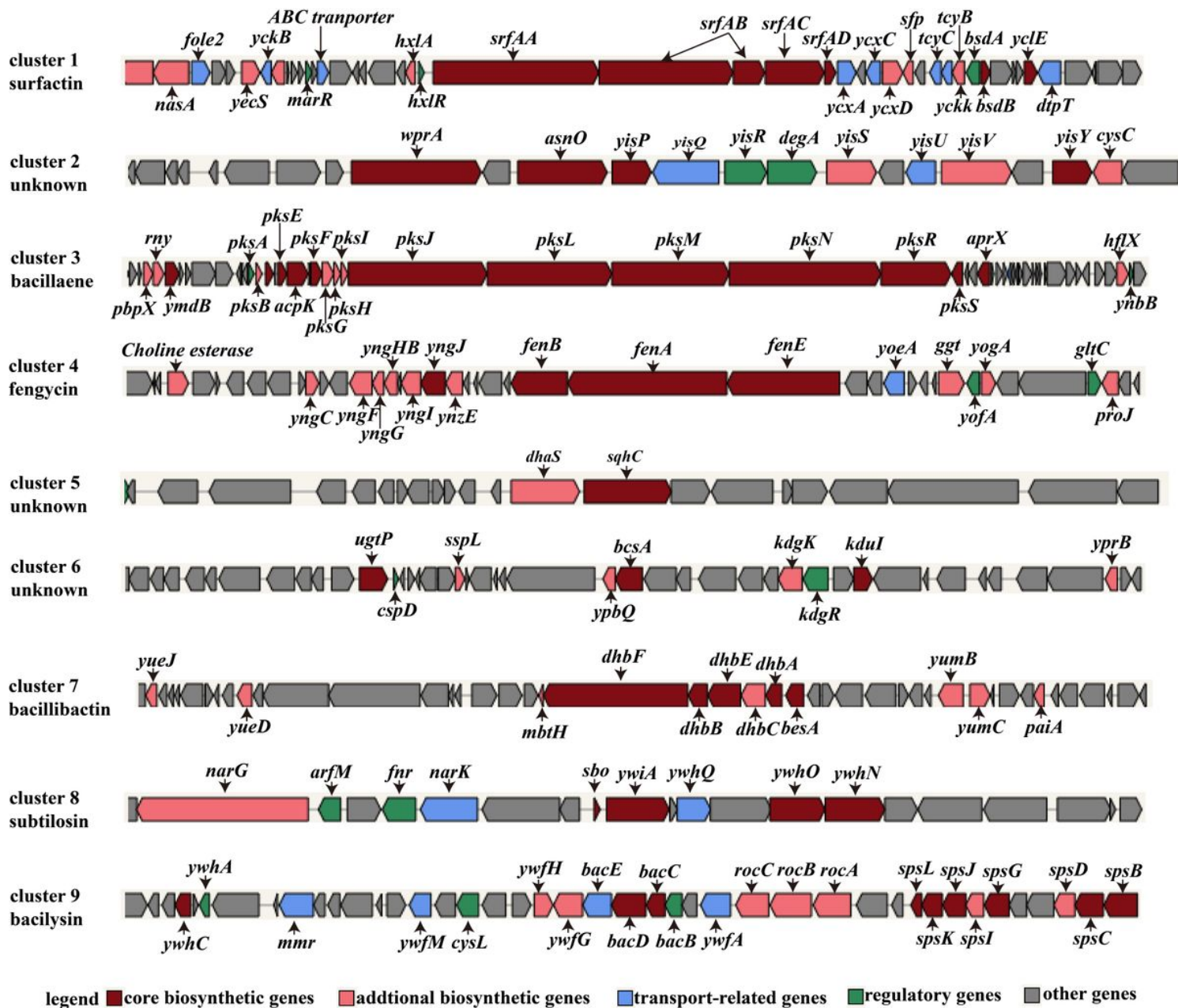
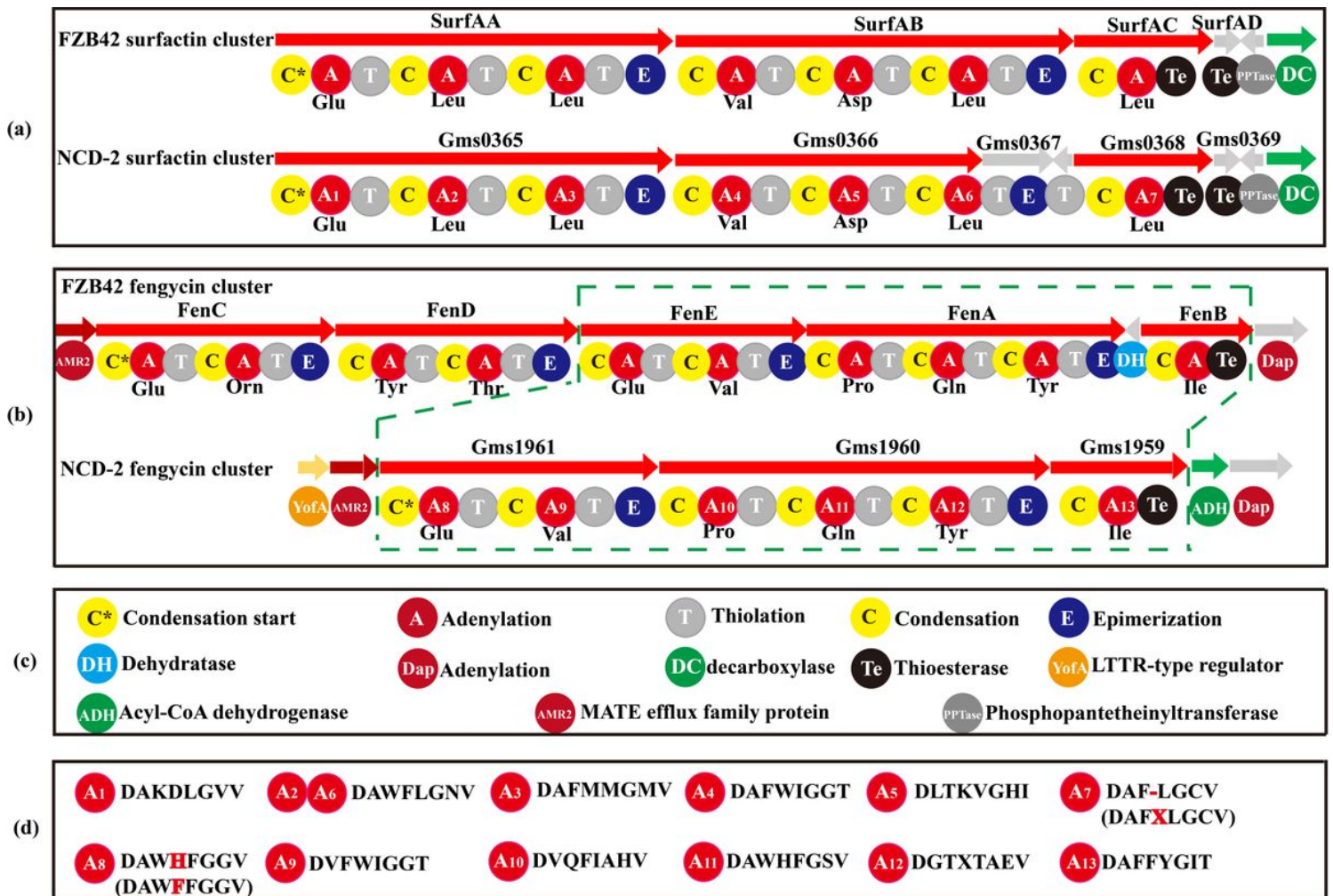


Figure 3

Schematic diagram of nine secondary metabolite biosynthetic gene clusters in *B. subtilis* strain NCD-2. antiSMASH was used to predict potential secondary metabolite biosynthetic gene clusters. Different color blocks represent genes with different functions; the genes marked with dark red, light red, blue, green, and gray are core biosynthetic, additional biosynthetic, transport-related, regulatory, other genes, respectively.



**Figure 4**

Comparisons of functional domains of core genes involved in synthesizing surfactin and fengycin in NCD-2. The functional domains of core genes of clusters 1 (a) and 3 (b) in *B. subtilis* NCD-2. (c) The abbreviations indicate the functions of the corresponding structural domains. (d) The conserved binding pockets for substrates formed by amino acids in different adenylation domains.

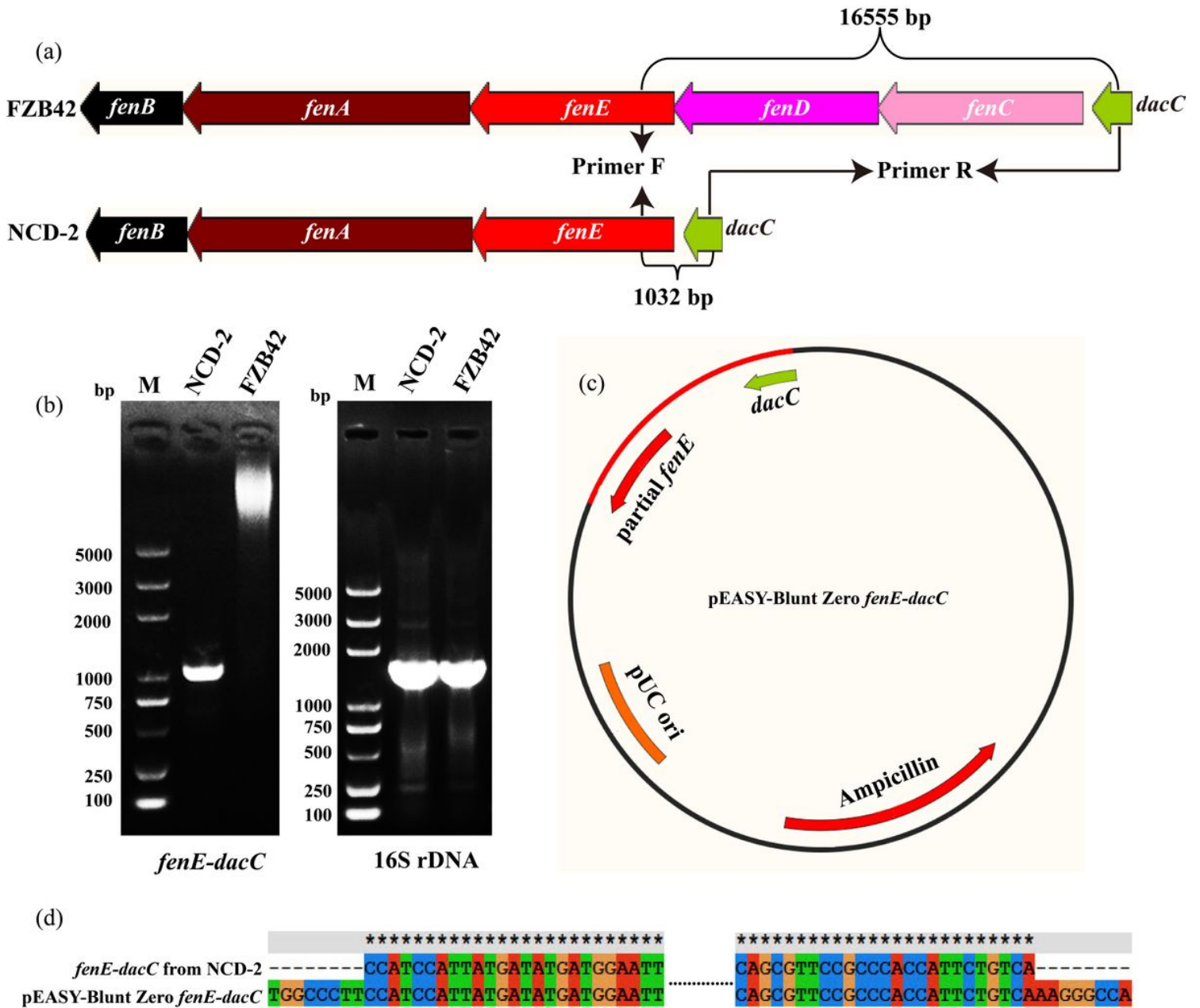


**Figure 5**

PCR and sequence of fragment between *fenE* and *dacC*. (a) Schematic diagram of designing primers according to conserved bases from NCD-2 and *B. velezensis* FZB42, (b) PCR of fragment *fenE-dacC* using genomic template NCD-2 and FZB42, the 16S rDNA was internal reference control, (c) Schematic diagram of constructed sequencing vector by ligating fragment *fenE-dacC* to pEASY-Blunt Zero vector, (d) blast of fragment *fenE-dacC* from NCD-2 and pEASY-Blunt Zero *fenE-dacC*, the two sequences about *fenE-dacC* were complete same.

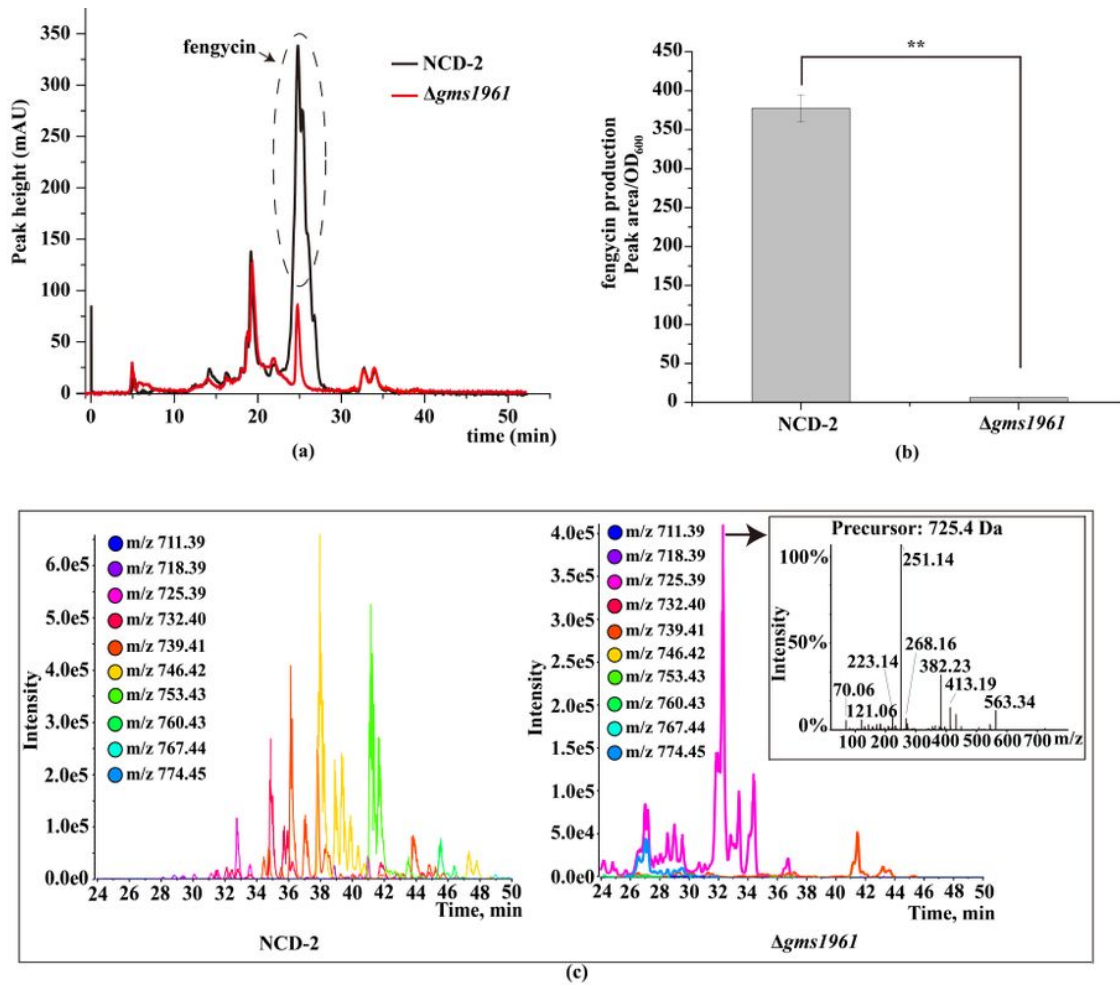


**Figure 6**

The role of *gms1961* in synthesizing fengycin. (a) FPLC of lipopeptides of strain NCD-2 and  $\Delta gms1961$ , (b) Quantitative production of fengycin in strain NCD-2 and  $\Delta gms1961$ , error bars represent standard deviation; asterisks depict significant differences as measured by t-test (\*\* $p < 0.01$ ), (c) Extract Ions Using Dialog (XIC) and UHPLC-QTOF-MS of fengycin from NCD-2 and  $\Delta gms1961$ . The lipopeptide fengycin showed different at 25-50 min between strain NCD-2 and  $\Delta gms1961$ , only the precursor related to  $m/z$  725.4 was same (the light purple line), but the fragments was absolutely different from that of fengycin from strain NCD-2.

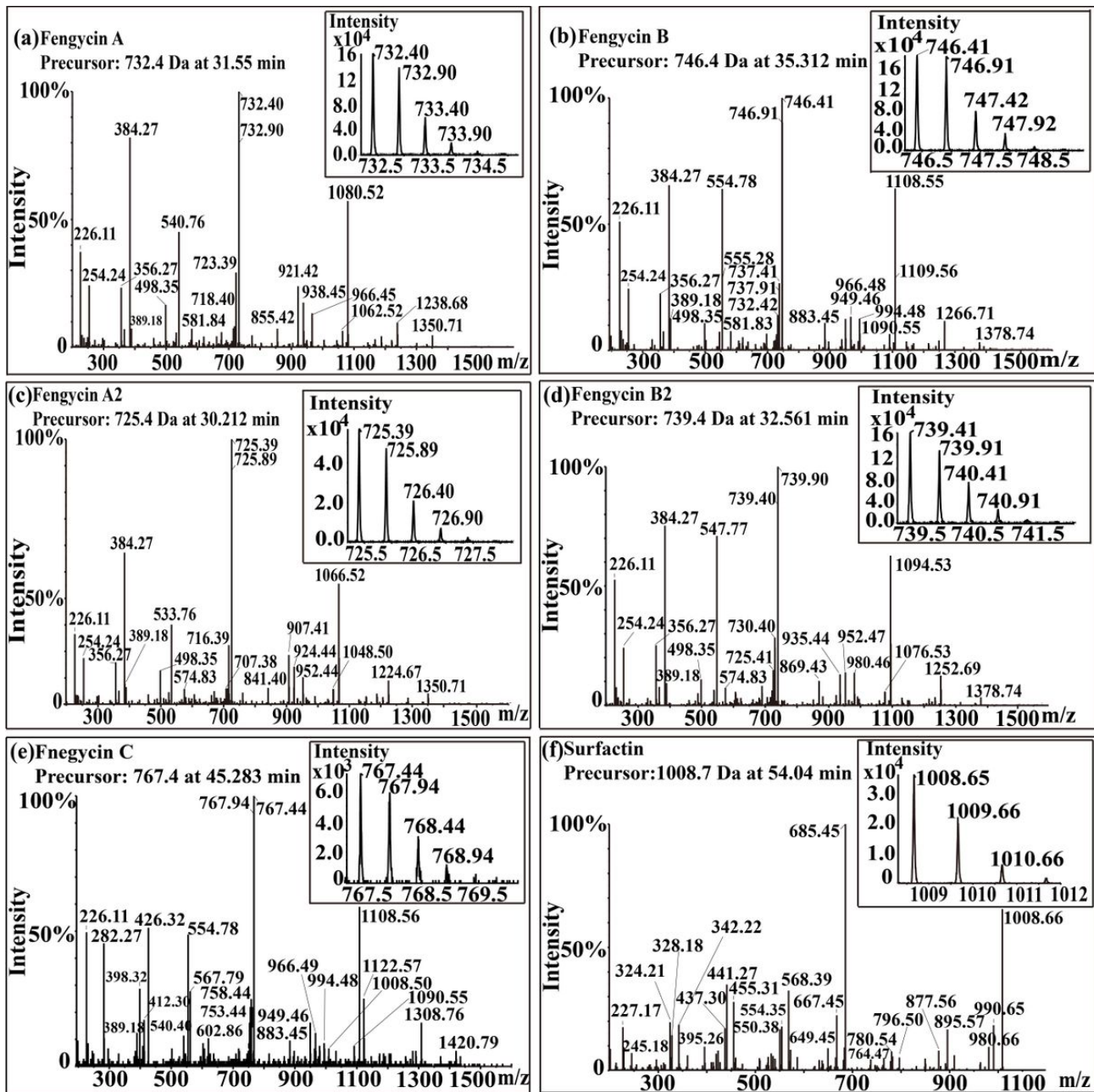
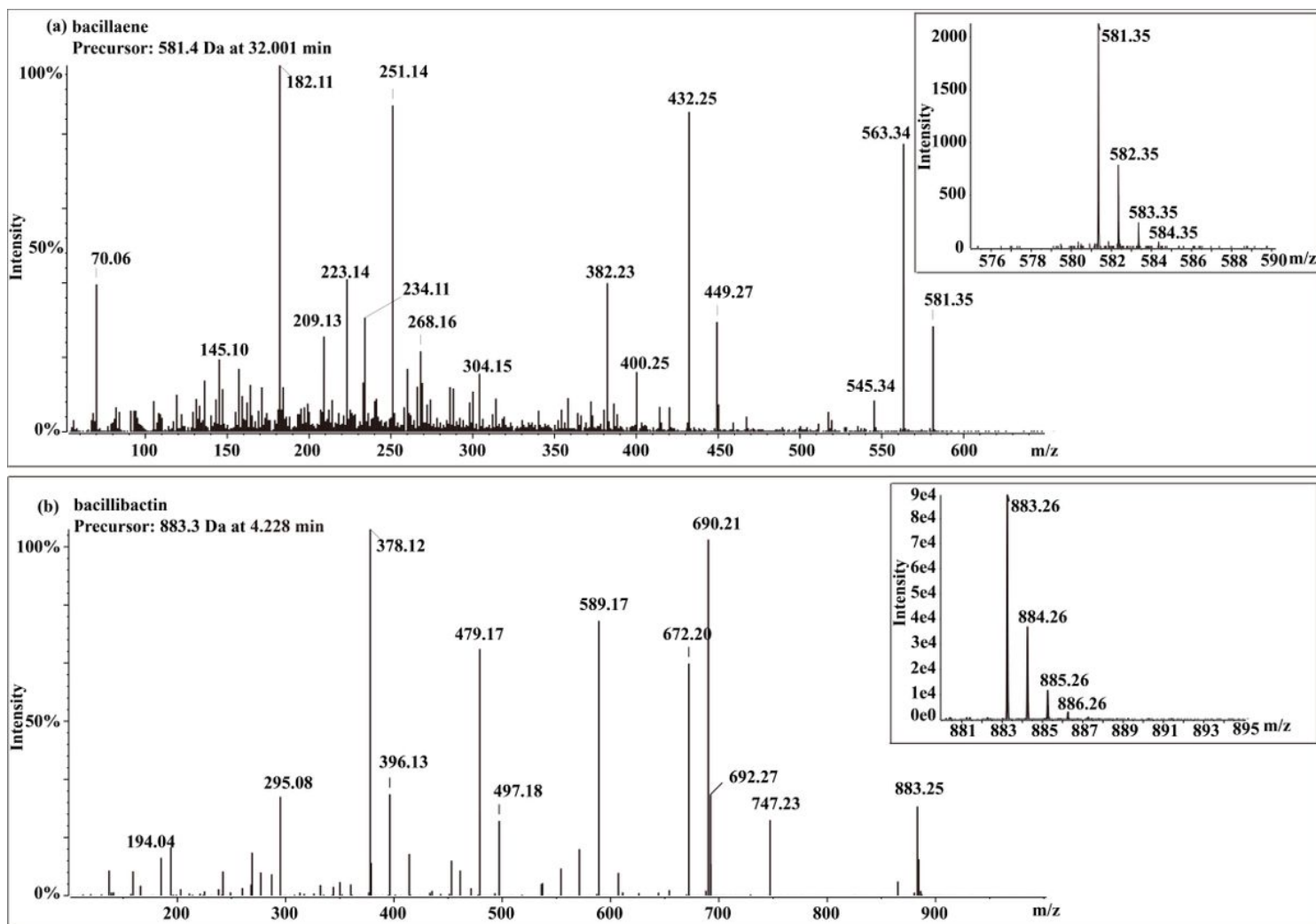


Figure 7

MS/MS spectra of protonated cyclic fengycin and surfactin ions. (a) m/z 732.4, (b) m/z 746.4, (c) m/z 725.4, (d) m/z 739.4, (e) m/z 767.4, and (f) m/z 1,008.7.



**Figure 8**

MS/MS spectra of protonated cyclic bacillaene and bacillibactin ions. (a) m/z 581.4, (b) m/z 883.3.

## Supplementary Files

This is a list of supplementary files associated with this preprint. Click to download.

- [Fig.S1.jpg](#)
- [Fig.S2.jpg](#)
- [Fig.S3.jpg](#)
- [Fig.S4.jpg](#)
- [Fig.S5.jpg](#)
- [Fig.S6.jpg](#)
- [Fig.S7.jpg](#)
- [Fig.S8.jpg](#)
- [Fig.S9.jpg](#)
- [Fig.S10.jpg](#)